ABSTRACT

Title of Thesis:	HYGROSCOPICITY OF CHOLESTEROL IN VARIOUS ORGANIC SOLVENTS
Author:	Farima Barati, Master of Science, 2018
Thesis Directed By:	Associate Professor, Akua Asa-Awuku, Department of Chemical and Biomolecular Engineering

Organic aerosols and partially soluble particles can uptake water, form droplets and act as cloud condensation nuclei (CCN). Cholesterol is a well-known organic aerosol. Cholesterol is insoluble in water (<0.002 *gram* in 100 *ml* of H_2O) but dissolves in organic solvents. In this study, we examine the ability of cholesterol generated in three dilutions of 3 alcohols (ethanol, isopropanol and acetone) to act as CCN. The apparent hygroscopicity, κ, varies over two orders of magnitude, from ~ 0.001 to 0.1. We use statistical analysis of variance (ANOVA) to define significant physical and chemical factors that modify κ. Results show that as volume of water increases, κ changes. However, the type of alcohol does not significantly modify the hygroscopicity. Increases in alcohol concentration decrease droplet surface tension and change aerosol shape. Thus, the apparent κ is corrected with surface tension and shape factor data and estimated to be ~0.028 ± 0.02.

HYGROSCOPICITY OF CHOLESTEROL IN VARIOUS ORGANIC SOLVENTS

by

Farima Barati

Thesis submitted to the Faculty of the Graduate School of the
University of Maryland, College Park, in partial fulfillment
of the requirements for the degree of
Master of Science
2018

Advisory Committee:
Professor Akua Asa- Awuku, Chair
Professor Richard V. Calabrese
Professor Amy J. Karlsson

Acknowledgements

Foremost, I would like to express my sincere gratitude to my advisor Professor Akua Asa- Awuku for giving me the opportunity to work in her research group, for her support, patience and immense knowledge.

Besides my advisor, I also appreciate the help and advice of the members of this research group: Qi Yao, Emmanuel Fofie, Patricia Razafindrambinina and Francis Oyebajo.

Finally, I would like to acknowledge my friends and family for their support of this endeavor. Thanks are due to my mother, father and my brother.

Table of Contents

List of Tables

List of Figures

List of Abbreviations

CCN- Cloud Condensation Nuclei

CN- Condensation Nuclei

PM- Particulate Matter

EPA- Environmental Protection Agency

SMCA- Scanning Mobility CCN Analysis

DMA- Differential Mobility Analyzer

TDMA- Tandem Differential Mobility Analyzer

AAC- Aerodynamic Aerosol Classifier

CPC- Condensation Particle Counter

OPC- Optical Particle Counter

SMPS- Scanning Mobility Particle Sizer

APS- Aerodynamic Particle Sizer

TEOM- Tapered Element Oscillating Microbalance

MOUDI- Micro Orifice Uniform Deposit Impactor

Chapter 1: Introduction

Aerosols emitted from cooking and specifically meat cooking have always been considered due to their important contribution to atmospheric pollution. Aerosols form droplets in atmosphere when exposed to supersaturated amounts of water vapor. Hence, aerosol can act as cloud condensation nuclei (CCN), indirectly impacting climate by influencing cloud lifetime and precipitation [1,2]. Particles also affect air quality, visibility and human health. Especially, particles smaller than 2.5μm known as $PM_{2.5}$ have been reported to cause the highest mortality rate due to the simple penetration to lungs [3]. The ability of particles to uptake water and become CCN is controlled by foremost particle size and then particle chemistry [4].

The particle mass distribution of various sources of emissions (including cooking) has shown that the peak mass occurs in diameters lower than 0.2 μm. For example, published work examined emissions from a hamburger and compared the aerosol composition of fried and charbroiled emissions [5]. Cholesterol has a significant rate of emissions in the US and needs further attention [6].

In this chapter, we provide a general overview of the major topics of this study (Aerosols in clouds, Aerosols in Air Pollution and Subsequent Health Effects). Lastly, an overview of the objectives of the thesis and motivation are provided.

1.1. Clouds

Atmosphere is an important part of living creatures' lives. Human beings constantly interact with the atmosphere. Although human activities are not the only determining factor in air quality, anthropogenic sources play a significantly important

role in what goes into the atmosphere. Better air quality means more healthy people both physically and mentally with higher life expectancies. Mutually, daily human life generates several particles with different properties and lifetimes directly into the air. Every task we do, we are in fact generating some particles into the atmosphere that may result in climate effects, impacts on clouds, their lifetime and precipitation and many other human-made modifications. Cloud formations is principally based on buoyant forces and water vapor existence can suffer from difficulties caused by anthropogenic sources.

Clouds and their lifetime and precipitation have important effects in global climate. Clouds have always been taken as one of the clearest signs for weather forecasting [7]. Based on NASA report [7], existence of scattered white cumulus clusters stagnant in a blue sky give us an idea of having a dry sunny day. Massive dark clouds remind us of rain and thunderstorm. Red colored clouds in sky are mostly a hint of a snow in the following day. Currently, weather forecasting based on clouds is performed with a high accuracy and based on developed technologies.

The most valuable key role of clouds in determining the climate is balancing Earth's radiation and precipitating. NASA has described the principals perfectly which I summarize them in brief[8]. To balance the energy in the atmosphere, energy released from sun and the energy radiated from Earth should satisfy conservation of energy. Clouds are vital to control the heat reaching the Earth because of the amount of sunlight they reflect. Except clouds, the entire atmosphere is almost transparent to solar radiation. Studies show that surface absorbs likely about 70 percent of the total sunlight reaching the Earth’s atmosphere. They also influence heat released by Earth since they inhibit

these radiations. Rains and snows precipitations release a significant amount of heat to the atmosphere as well. Thus, it is understood that if any activity can make changes to clouds, it will eventually perturb the atmosphere global energy [8].

The formation of clouds take place when water vapor available in the atmosphere is cooled and condensed on airborne particles. There are many compounds that provide this surface for water vapor to condense on. These clouds are called cloud condensation nuclei or CCN which we would discuss more detailed further. CCN can be made of organic or inorganic compounds or even a mix of them. Sulfate particles are among the most popular compounds forming clouds.

1.2. Aerosol and Air Pollution

An aerosol is a suspension of solid particles or liquid droplets, in air or another gas. Aerosols can be produced from natural or anthropogenic sources. Examples of natural aerosols can be fog, dust and geyser steam. Haze, smoke and particulate air pollutants are tangible examples of pollutants made from anthropogenic activities. Black carbon is a pollutant emitted from vehicles and plants which is a popular topic to study nowadays. Its ability to form droplets and how to mitigate its concentration in the atmosphere is of high interest. Aerosols also have a few other sources including agricultural sources such as solute composition, mixed biogenic sources such as gas-phase effects and of course vehicle emissions [9].

Airborne pollutants are considered to have various phases. Gas phase is related to popular pollutants like O_2, CO_2, NO_x and hydrocarbons. Aerosols are classified into two categories of primary aerosols and secondary aerosols. Primary pollutants are designated as particles that get into environment directly while secondary pollutants are consequence

of reactions between distinct gas phase pollutants [10]. It is known by public that reduction in primary pollutant emissions will lead to decrease in rate of secondary pollutant concentration in ambient. While this is not true based on data collected. For example, it has been illustrated that not only ozone and nitrogen concentration are not proportional but also, they act in reverse of each other [11].

Ambient aerosol is of great importance when it comes to study atmosphere. This is because of its considerable impacts on visibility, global climate and atmospheric chemistry [12]. Aerosols affect air quality and climate both directly and indirectly. Aerosols provide nuclei for cloud droplets to condense on. In other words, cloud condensation nuclei or CCN are the particles that will absorb water vapor in the atmosphere and form droplets. High concentration of these droplets will form clouds. The clouds formed will be brighter and increase the albedo (reflection of light). Small droplets forming clouds are not capable of proper coalescence and so fewer number of raindrops are formed which will lead to longer lifetime of clouds. Hence, the properties of CCNs can modify cloud properties like precipitation or lifetime. When there is high concentration of CCN, there would be greater albedo in atmosphere that will conclude in cooling effect. This is where size matters since smaller particles reflect more. This cooling effect is not a negligible amount due to proof of the fact that clouds account for almost 50% of planetary albedo. Small changes in clouds yield large changes in global energy balance. Thus, we understand that people both cause global warming and cooling. It is worth to mention that, these effects on climate are still countering significant uncertainty. There are some climate models to predict anthropogenic activities impact, however, they are based on remarkable assumptions [13].

Air pollution is one of the main reasons for diseases, health costs and mortality. We may never pay attention to the particles entering the air by just a normal barbeque picnic. You may never think of sea salt influencing the air quality. Air pollution is a topic that everyone has heard about it while most of us immediately think of this concept as emissions produced from plants and cars. Of course, the products of fossil-fuel are the major source, however, air pollution comes from various sources. Overall, pollutants are classified by their source of generation, size, chemical composition, and whether they are emitted into indoor or outdoor environments.

The Clean Air Act requires EPA to define six typical pollutants as criteria pollutants: ground-level ozone, particulate matter, carbon monoxide, sulfur dioxide, lead and nitrogen [14]. Based on EPA report mentioned, compounds of this group can cause harmful effects on air quality as well as human beings. Particulate matter corresponds to particles that have the size less than ten micrometer. These particles can penetrate the lungs, liver and kidney because of their tiny size and cause diseases such as cancer.

1.3. Health Effects

The ability of aerosol to uptake water has the potential to impact both climate and health. Inhalation of condensed water that now we know may contain other harmful particles as CCN can cause health effects and especially effects on our lungs. These particles are in sizes below 10nm and can go deep into lungs causing respiratory issues. Hygroscopicity of particles is important from a different view as well. Dry particles available in out lung tract are exposed to relative humidity. Therefore, they can absorb water and start to grow to larger sizes which would cause harm and infection to our body [15].

In general, adverse respiratory symptoms and diseases such as asthma, allergy and coughing remind us of air pollution issues. Studies show that ozone increases airway inflammation and causes body responses to inhaled allergens. It also has been reported that ozone acts as a reason for increased risk of asthma among children in California playing outdoor sports. Nitrogen oxides has been related to intensify respiratory infection and inhaled allergen responses. Long exposure to sulfur dioxide (SO_2) in high concentrations especially during exercise create respiratory irritations. In terms of emergency, SO_2, sulfates, and acid aerosols have been reported to bring on emergency visits to hospitals due to severe asthma problems.

Particulate matter or PM are suspended particles that are divided into three groups. First group consists of coarse PM or PM_{10} with an aerodynamic diameter in the range of 2.5-10 mm. They can be found in abraded soil, road dust, construction debris, or aggregation of smaller combustion particles. Fine PM or $PM_{2.5}$are particle with a size of less than 2.5 mm in diameter and ultrafine PM is even smaller then 0.1mm. The last two groups are basically generated from the combustion of fossil fuel products. The US Environmental Protection Agency (EPA) has set regulations and limit standards for $PM_{2.5}$ and PM_{10} but not any regulations for ultrafine PM. However, ultrafine PM happens to be more toxic due to availability of transition metals and redox cycling chemicals, and not compliant with mass standard monitoring [16].

1.4. Cholesterol

Cholesterol is a sterol type of organic compounds. It is also a lipid molecule found in animal cells. It has the chemical formula of $C_{27}H_{46}O$ and a white crystalized powdery appearance. The structure of the molecule is shown in Figure 1.1.

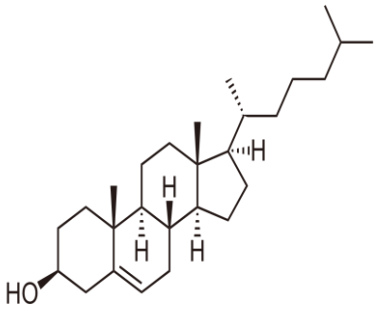

Figure 1.1. Structure of cholesterol (picture taken from Wikipedia)

Cholesterol is an indivisible part of any food we eat and especially meat. Hence, cooking and specifically meat cooking emits cholesterol particles substantially into the atmosphere. Later, these particles can act as CCN and affect our climate. That is why we can consider cholesterol as a pollutant although it is not among the known and obvious pollutants [17].

Cholesterol is an insoluble organic species with a solubility of less than 0.002 *gram* in 100 *ml* water [18]. This is one of the reasons little research has been focused on cholesterol corresponding to air quality. Although cholesterol cannot be dissolved in water, it has a good solubility in alcohols such as acetonitrile, isopropanol, methanol, ethanol, acetone and their mixtures with water. In this study, we explore the impact of volume ratios of water to three different alcohols: ethanol, isopropanol and acetone. Among these three solvents, acetone and ethanol have the same solubility but different boiling points while isopropanol has the highest solubility and boiling point [19]. Thereby, adding alcohol to water is a method for preparing solutions of cholesterol for further experiments.

1.5. Goals and Objectives

Various characteristics of particles have been studied. Hygroscopicity of aerosols is among the characteristics that play important role in determining global climate. While variety of experiments have been conducted with the aim of understanding different compounds water intake ability, organics and insoluble materials have not been extensively researched due to their complexity [20]. There are plenty of organic compounds in the atmosphere that are known as an insoluble category. However, they have an approximate solubility of $10^{-5} \pm 10^{-2} M$ that enable them to be available as solutes near critical radius [21]. Thereby, these compounds cannot be neglected. This concept also happens to be of great importance since there are several insoluble compounds such as black carbon emitted with a high concentration to atmosphere.

CCN droplet experimentation and theory has advanced in the past decade. Specifically, rapid high-resolution CCN measurements have improved the precision of reported CCN critical diameters. Furthermore, particle morphology and effective density are known to influence reported values [22] and the use of pendant drop surface tension measurements can support inferences about depressions of surface tension on the droplet at activation.

In this study, we a) further explore the contribution of insoluble organic cholesterol to CCN number and b) assess the impact of organic solvents used to modify CCN activity. Specifically, the volume ratios of organic solvent in water of three different alcohols (ethanol, isopropanol and acetone) strategically selected for their range in solubility and boiling points are varied. We then report CCN activation regarding apparent supersaturated κ-hygroscopicity, and quantify sources of variance (shape factor,

surface tension, experimental drying techniques) in reported values with analysis of variance (ANOVA) statistics. The current work focuses on cholesterol, an insoluble compound found considerably from meat cooking emissions. In terms of CCN activity, cholesterol can act as CCN when reaching atmosphere. Thereby, it has significant impacts on air quality and clouds. The goal of this project is to learn about factors plying role in cholesterol's hygroscopicity when dissolved in organic solvents.

1.6. Layout of Thesis

The following is a list of items discussed in this thesis.

- Chapter 1 introduces the scientific concept of cloud formation, the importance of aerosols, the effects of CCN activation in global climate and health and eventually the justification for this study.
- Chapter 2 reviews detailed description about Kohler theory and shape factor equations. Then, general information about instruments and their functionality is provided.
- Chapter 3 provides a literature review and summarizes the current state of
- knowledge about droplet formation of organic and inorganic compounds, various techniques performed,
- Chapter 4 covers experimental setups, materials and methods that were used in each section aiming for a specific goal.
- Chapter 5 discusses the results of κ values calculated with two methods. Based on the κ values analysis, shape factor and surface tension are measured to correct κ values and assay morphology and surface tension influences on cholesterol hygroscopicity.

- Chapter 6 includes conclusions made by analyzing the results found in this study and discusses future work needed to be done in this field.

Chapter 2: Theoretical Background

This chapter discusses the basic knowledge about theories and instruments used further to obtain results. First, Kohler Theory, κ parameter and importance of surface tension are explained. The equations required for κ calculation is also provided. Later the concept of shape factor is covered in addition to corresponding equations. In the last section of this chapter, details of instruments operation are provided. Further in this study, we test two of the most important activation assumptions (constant surface tension and spherical particle size) for insoluble cholesterol generated from dilute alcohol solvents.

2.1. Köhler Theory and Single Parameter Hygroscopicity κ

To determine hygroscopicity, κ values are calculated and compared in all the different samples of the mixtures. κ value can be derived using Kohler Theory. This parameter is defined to simplify determining hygroscopicity quantitatively. Kohler Theory is based on thermodynamic equilibrium including two major laws: Kelvin law to consider curvature and Raoult law to count for solute terms. This theory can provide us the supersaturation ratio. First, we need to understand how the Kelvin effect equation is derived. Kelvin effect is essentially the equilibrium vapor pressure over a curved surface. Our approach is to figure out the change in Gibbs energy during the formation of droplet. The whole derivation is taken from the book "Atmospheric chemistry and physics: from air pollution to climate change" [23]. Thus:

$$\Delta G = G_{droplet} - G_{pure\ water} \quad (1)$$

The number of vapor molecules available after the droplet is formed will be denoted as N_1 which is equal to $N_T - n$ where N_T is the initial total number of vapor molecules and n is obviously number of molecules forming the droplet. If we indicate the Gibbs free energy of a molecule in vapor phase with g_v and in liquid phase with g_l then Equation (1) will simplify to:

$$\Delta G = N_1 g_v + n g_l + 4\pi {R_p}^2 \sigma - N_T g_v \quad (2)$$

where σ is the surface tension and the $4\pi {R_p}^2 \sigma$ term is considering the energy caused by curvature. Substituting definition of $N_T = n + N_1$ and $n = \frac{4\pi {R_p}^3}{3v_l}$, where v_l is the liquid volume, provides Equation (3):

$$\Delta G = \frac{4\pi {R_p}^3}{3v_l}(g_v - g_l) + 4\pi {R_p}^2 \sigma \quad (3)$$

Next step, it is necessary to describe $(g_v - g_l)$. From thermodynamics, we know that in general Gibbs free energy accounts for heat, work and flux of particles:

$$dG = -SdT + VdP + \Sigma \mu_i dn_i \quad (4)$$

Assuming constant temperature and $dn_i = 0$ results in $dG = VdP$.So, this expression can be used to simplify $g_l - g_v = (v_l - v_v)dP$. Since $v_l \ll v_v$, and assuming ideal gas condition for the vapor phase ($v_v = \frac{KT}{P}$), we end up at Equation (5):

$$g_l - g_v = -KT \int_{P_A^\circ}^{P_A} \frac{dP}{P} \Rightarrow g_l - g_v = -KT Ln\left(\frac{P_A}{P_A^\circ}\right) \quad (5)$$

where P_A° stands for vapor pressure for pure *A* and P_A is the actual equilibrium vapor pressure of *A* over liquid. The ratio of $\frac{P_A}{P_A^\circ}$ provides the definition of supersaturation (S). Combination of (5) and (3) using supersaturation definition results in the following equation:

$$\Delta G = -\frac{4\pi {R_p}^3}{3v_l} KTLn(S) + 4\pi {R_p}^2 \sigma_{\frac{s}{a}} \quad (6)$$

It can be deduced from this expression that supersaturation equal to one can act as a boundary. In supersaturations lower than one, both terms on the left-hand side of Equation (6) will increase and so the Gibbs free energy. However, in situations with $S > 1$, Gibbs free energy increases due to the increase in both terms in low radiuses. Later and in higher radiuses, the influence of first term related to solute effects is greater than curvature effects in determining Gibbs energy. Thus, Gibbs energy starts to decrease at a certain radius denoted as R_p^*. To find this parameter, we should put the derivative of Equation (6) with respect to R_p equal to zero.

$$R_p^* = \frac{2\sigma_{\frac{s}{a}} v_l}{KTLnS} \quad (7)$$

Consequently, Kelvin effect can be expressed in terms of supersaturation parameter:

$$S = \exp\left(\frac{2\sigma_{\frac{s}{a}} M}{KTR_p\rho_l}\right) \quad (8)$$

Or

$$P_A = P_A^{\circ} \exp\left(\frac{2\sigma_{\frac{s}{a}} M}{KTR_p\rho_l}\right) \quad (9)$$

The main conclusion made by Kelvin effect is that the vapor pressure is significantly higher over a curved rather than a flat surface.

With having Kelvin effect expression in mind, we should derive κ equation which is essentially the basis of the project. We are aiming for finding the vapor pressure of water (P_w) over vapor pressure of solute (P_s). From Equation (9) and the definition for pressure of solute which is $P_s = \gamma_w x_w P^{\circ}$, we get:

$$\frac{P_w}{\gamma_w x_w P^\circ} = \exp\left(\frac{4\sigma_s v_l}{\frac{\bar{a}}{KTD_p}}\right) (10)$$

where, $x_w = \frac{n_w}{n_w + n_s}$ is the molar fraction of water in the solution.

$$\frac{\pi D_p{}^3}{6} = n_w v_w + n_s v_s \ (11)$$

Using Equation (11) helps us to come up with an expression for x_w to substitute in (10):

$$\frac{1}{x_w} = 1 + \frac{n_s}{n_w} = 1 + \frac{n_s v_w}{\frac{\pi D_p{}^3}{6} - n_s v_s} \ (12)$$

Now, we substitute (12) in (10) and apply logarithm to it:

$$Ln\left(\frac{P_w}{P^\circ}\right) = \left(\frac{4\sigma_s v_l}{\frac{\bar{a}}{KTD_p}}\right) + Ln\gamma_w - Ln\left(1 + \frac{n_s v_w}{\frac{\pi D_p{}^3}{6} - n_s v_s}\right) (13)$$

For a dilute solution, we can set following assumptions:

$$n_s v_s \ll \frac{\pi D_p{}^3}{6}$$

$$\gamma_w \longrightarrow 1$$

Also, we can use the definition of $Ln(1 + x) \simeq x$ for the third term on the left-hand side of Equation (13). Applying these simplifications will lead to:

$$Ln\left(\frac{P_w}{P^\circ}\right) = \left(\frac{4\sigma_s V_l}{\frac{\bar{a}}{KTD_p}}\right) - \frac{6 n_s V_w}{\pi D_p{}^3} \ (14)$$

If we name the constant parameters, *A* for Kelvin effect and *B* for solute effects, Equation (14) can be written as:

$$Ln\left(\frac{P_w}{P^\circ}\right) = \left(\frac{A}{D_p}\right) - \frac{B}{D_p{}^3} \ (15)$$

where, we should keep it mind that $n_s = \frac{\nu \pi {d_s}^3 \rho_s}{6 M_s}$.

In other words, this equation can be expressed as:

$$\mathrm{LnS} = \left(\frac{\mathrm{A}}{\mathrm{D_p}}\right) - \frac{\mathrm{B}}{\mathrm{D_p}^3} \quad (16)$$

Next goal is to find critical point. First, we take the derivative of Equation (16) with respect to D_p and set it equal to zero.

$$\mathrm{D_{pc}} = (\frac{3\mathrm{B}}{\mathrm{A}})^{\frac{1}{2}} \quad (17)$$

where, D_{pc} is the critical particle diameter. Substituting this in (16) will provide us the critical supersaturation (S_c) value:

$$\mathrm{LnS_c} = (\frac{4\mathrm{A}^3}{27\mathrm{B}})^{\frac{1}{2}} = \mathrm{LnS_c} = (\frac{4\mathrm{A}^3\rho_w\mathrm{M_s}}{27\nu\rho_s\mathrm{M_w}\mathrm{d_s^3}})^{\frac{1}{2}} \quad (18)$$

The parameter κ is designed to ease hygroscopicity measurements based on Equation (18).

$$\kappa = \frac{\nu\rho_s\mathrm{M_w}}{\rho_w\mathrm{M_s}} = \frac{4\mathrm{A}^3}{27\,\mathrm{D_d^3}\ln^2\mathrm{S_c}},\ \mathrm{A} = \frac{4\sigma_{\frac{s}{a}}\mathrm{M_w}}{\mathrm{RT}\rho_w} \quad (19)$$

where, D_d is the dry diameter, S_c is critical supersaturation, $\sigma_{\frac{s}{a}}$ is the surface tension between air and solution, ρ_s density of solvent, ν is the disociassion factor and ρ_w is density of water [23].

Theoretical κ is calculated using the second term of Equation (19) which only depends on compound physical and chemical properties. But experimentally, dry diameter and supersaturation are required to be substituted into the third term of Equation (19) to calculate apparent κ which typically ranges from 0 to 1.2. Higher κ defines higher hygroscopicity. When κ is equal to zero, the particle is only wetting by pure water. κ values higher than zero but less than 0.01 corresponds to chemically aged particles and insoluble particles. Particles with κ values higher but still less than 0.5 are moderately hygroscopic organic species. Most of inorganics possess a κ value equal to one [24]

To measure κ experimentally, two sets of instruments are operated based on aerodynamic diameter and mobility diameter. First setup is running SMCA or scanning mobility CCN analysis with Moore et al. method which will be discussed further [25]. Performing analysis of variance indicates that changing the solvent is not influencing results and the ratio of alcohol to water is the major factor. Later, shape factor is calculated to determine the effect of shape of cholesterol in the results using Tavakoli method [26]. Results lead to approving the differences in κ values and shape factors when changing the amount of water. Surface tension is then measured by optical tensiometer to verify the hypothesis that surface tension is the modifying factor.

$\sigma_{s/a}$ and D_d are both scaled to the third power in κ-Kohler theory and can contribute large uncertainties to $\kappa_{apparent}$ values [27], [28].

2.2. Shape Factor

The deviation of non-spherical CCN can be accounted for with particle shape factor information [29]. Drag force on a particle is calculated using Stokes' law assuming particles to be spherical:

$$\mathrm{F_D} = \frac{3\mu\pi \mathrm{V D_v}}{\mathrm{C(D_v)}} \quad (20)$$

where, μ is gas viscosity and D_{ve} is volume equivalent diameter. $C(d)$ is the Cunningham slip correction factor corresponding to the given diameter:

$$\mathrm{C} = 1 + \left(2\frac{\lambda}{\mathrm{d}}\right)\left(1.142 + 0.558\mathrm{EXP}\left((-0.999)\frac{\mathrm{d}}{2}\lambda\right)\right) \quad (21)$$

where, λ is the mean free path which is equal to 65 [30].

For non-spherical particles, we should consider a drag correction factor called dynamic shape factor. Shape factor is generally described as the ratio of drag force on a

non-spherical particle to drag force on the spherical particle which has the same volume (based on volume equivalent diameter):

$$\text{shape factor} = \chi = \frac{F_D}{F_{Dve}} = \frac{D_{mo} * C_{Dve}}{D_{ve} * C_{Dmo}} \quad ; D_{ve} = \left(\frac{D_{ae}^2 D_{mo} C_{D_{ae}}}{\rho C_{D_{mo}}}\right) \quad (22)$$

where, D_{ve} is the volume equivalent diameter, D_{mo} is the electrical mobility diameter and D_{ae} is the aerodynamic diameter.

Shape factor is in fact expressed as a function of Knudsen number which is quantitatively the ratio of mean free path of gas to radius of particle $(\frac{\lambda}{d})$ which is apparently used in the equation in the Cunningham correction factor. The Knudsen number is a representative of the state of the fluid dynamics, whether it is statistical mechanics or the continuum mechanics. Knudsen number greater than one means statistical dynamics should be considered so that the mean free path of a molecule is on the order of length scale of the situation.

Shape factor of a sphere is equal to one. There are different shapes a particle can obtain. Figure 2.1 indicates various type of particles with varied shape factors. Hence, the deviation of the shape factor value from one is essentially the deviation of the particle morphology from a sphere. Most of the particles contain shape factors greater than one. The physical meaning is that the particle can settle in air slower than the spherical one with equal volume [30]. There are also particles with lower than one shape factor especially in larger diameters which is due to the fact that particles with larger diameters do not stick to each other, cannot maintain the compact structure and so act more chain-like or streamlined objects [29].

Table 1
Summary of different particle types and associated relations of particle density, material density, and shape factor

	Particle type	Diameter relations	ρ_p and ρ_m relations	χ and χ' relations
A	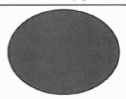 Sphere (no voids)	$d_{me} = d_{ve}$ $d_m = d_{ve}$ $\frac{d_{ve}\rho_0}{\rho_p} = d_{ve}$	$\rho_p = \rho_m$	$\chi = \chi' = 1$
B	 Sphere (internal voids)	$d_{me} = d_{me} * \delta$ $d_m = d_{ve}$ $\frac{d_{ve}\rho_0}{\rho_p} = d_{ve}$	$\rho_p < \rho_m$ $\delta^3\rho_p = \rho_m$	$\chi = 1$ $\chi' = \delta\frac{Cc(d_{me})}{Cc(\delta \cdot d_{me})}$
C	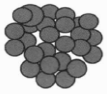 Compact Aggregate (internal voids)	$d_{me} = d_{me} * \delta$ Assume: $d_m \approx d_{ve}$	$\rho_p < \rho_m$ $\delta^3\rho_p = \rho_m$	$\chi \approx 1$ $\chi' = \delta\frac{Cc(d_{me})}{Cc(\delta \cdot d_{me})}$
D	 Irregular (no voids)	$d_{me} = d_{ve}$ $d_m > d_{ve}$	$\rho_p = \rho_m$	$\chi' = \chi > 1$
E	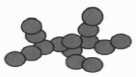 Aggregate (no voids)			
F	 Irregular (internal voids)			
G	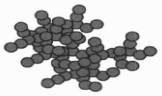 Aggregate (internal voids)	$d_{me} = d_{me} * \delta$ $d_m > d_{ve}$	$\rho_p < \rho_m$ $\delta^3\rho_p = \rho_m$	$\chi' > \chi > 1$ $\chi' = \chi \cdot \delta\frac{Cc(d_{me})}{Cc(\delta \cdot d_{me})}$

Reasonable assumptions about particle properties are also included.
Aggregate particles are a special case of irregular particles.

Figure 2.1. Morphology of particles. (Picture taken from reference [22])

2.3. Measurement Devices

Instruments are an inseparable part of every experiment. To understand experiments completely, one needs to get to know how the instruments function and what is the scientific rationale behind them. Below includes a brief description for each instrument used in this project.

The neutralizer is used to avoid charge effects on particles. It is functioning with Krypton 85. Krypton 85 is a radioisotope of Krypton. It is used in industry for various purposes including inspecting defects in an aircraft, ionizing sparks, measuring extruded films and testing leaks in semiconductors. One of the most common purposes is neutralizing electrostatically charged aerosols from nebulization, combustion, or powder dispersion.

The driers are made of silica gels. Silica gel is an amorphous and porous form of silicon dioxide, consisting of alternating silicon and oxygen atoms with nanometer-scale voids and pores. Silica gel is mostly known for its high water-absorption quality that enables it to dry or maintain a specific relative humidity. This advantage is because of silica gel high specific surface area (around 800 $\frac{m^2}{g}$) to absorb and keep water on its surface. In fact, this adsorption happens owing to the adsorption onto the surface of its numerous pores rather than by absorption into the bulk of the gel. It is also worth to mention that since our solutions contain organic solvents, it cannot function properly when using polycarbonate as driers since they may react. Thus, silica gels are the best option for the purpose of drying in this project.

The electrostatic classifier, including DMA or differential mobility analyzer works on the basis of electrical mobility. The electrical mobility applied on particles in the column, direct them to the end of column where they would exit. Particles move down the center of the column to avoid edge effects. The Hence, the instrument measures the particle electrical mobility. The point is that from using particles with known size, there is a size distribution based on electrical mobility. Thereby, the instrument will provide us the size distribution which is more desirable than electrical mobility for us. Also, this classifier includes a column for neutralizing particles to avoid charge effects before applying electrical mobility. To analyze the activation diameter, activation ratio is plotted versus particle dry diameter which should look like a sigmoid fit. However, we would observe two humps in the figure while the first one must happen below 0.2 activation. We literally ignore the first hump when attempting to add fits to the data collected. This is since the first hump corresponds to multiple charged particles.

CPC or condensation particle counter is the instrument used for counting the total number of particles. This instrument is using butanol to recognize particles. The condensation of butanol on particles will make them larger and easy to notice. Since butanol is a toxic compound and its inhalation especially causes headaches and dizziness, CPC requires a pump to ventilate the butanol emissions. Some versions of CPC have a pump inside and some need an external pump. Furthermore, all types of CPCs do not work with butanol and are water-based.

CCN counter or cloud condensation nuclei counter is utilized to measure concentration of condensed particles which are scientifically called activated particles. An important parameter for us is activation ratio defined as the ratio of concentration of CCN over total number of particles. This value is figured out by dividing the amount obtained from CCN to the CPC value. In terms of how this instrument functions, we should mention that particles are exposed to water vapor in the column and sheath flow that is basically recycled from sample flow. There is an optical particle counter (OPC) at the end of the column that measures the size distribution.

Aerodynamic aerosol classifier or AAC is another instrument for size selecting particles. AAC is dependent on aerodynamic diameter while DMA is based on electrical mobility diameter. This instrument provides size distribution by measuring settling velocity of particles.

Tensiometer is the instrument used to measure surface tension. Optical tensiometer is made up of a syringe and needle to create droplets and a camera to take photos of it and measure contact angles. The software used along with the instruments is “One Attension” and analyzes the surface tension of the droplet formed based on Young-Laplace law.

Chapter 3: Literature Review

This chapter provides an outline of the present state of knowledge of aerosols in two categories. First part is focused on various methods used for studying aerosol activation and ability to intake water. Third section covers literatures discussing particles morphology and surface tension that are two main factors in determining droplet forming potential of a particle.

3.1. Aerosol Activation Study Methods

Several instruments are needed to work individually or together to help us study aerosol dynamics deeply and in different areas. SMPS combined with APS is a sample of measuring size distribution by matching mobility diameter from SMPS and aerodynamic diameter found by APS. The two instruments are operated in parallel since neither of these instruments can cover a wide range of size distribution. They run experiments for low diameters with SMPS and APS for higher sizes. Later, with a simple algorithm using effective density (which is the ratio of density to shape factor), one size distribution is obtained. In Khlystov et al. paper, the goal is to convert size distribution of $PM_{2.5}$ to mass taking advantage of the combination of SMPS and APS. To verify this method, concurrent measurements from tapered element oscillating microbalance (TEOM) and micro orifice uniform deposit impactor (MOUDI) were compared. Results from SMPS and APS compared to TEOM outcome a shape factor of close to 1. MOUDI mass measurement data agree well with the method in size ranges between 0.1-2.5 μm while diameters lower than 0.1 μm indicated a little discrepancy [32].

Aerosols released into the atmosphere from cooking and food burning have been studied using the tandem differential mobility analyzer (TDMA) method. The growth ratio, size distribution and fraction of solubility of oily compounds such as Hollywood peanut oil, Mazola corn oil, Wesson canola oil, and Wesson vegetable oil have been calculated as well. The subsaturated droplet growth factor of long chain organic and oily compounds are close to 1. They mimicked the action of frying high-fat meats by using the type of oil desired into a pan and heated it electrically. Water droplets were dispensed on oil from a pipette with constant flow to make oil bubbles. Also, emissions from grilling Italian sausage has been measured. The comparison of results illustrate oil generated from frying action is greater than grilling. Subsaturated κ values are likely to be small [33].

The particle mass distribution of various sources of emissions has illustrated that there is a substantial difference in amount of submicron particles emitted whether they are fried or charbroiled. Charbroiling produces particles from oily species with a rate of 20-80 times higher [5]. Cholesterol has a very low solubility in water. Huff-Hartz et al, 2006 studied hygroscopicity of 19 limited solubility organic aerosols, including cholesterol. In these experiments, the solute was dissolved in aqueous and alcohol solutions to generate aerosol. The measurements were done at a fixed supersaturation equal to 1% using CCN counter and CPC to measure activation ratio and critical diameter [34].

3.2. Organic Aerosol Hygroscopicity

Organic aerosol (OA) is a major fraction of atmospheric aerosol [35]. The majority of OA that are known to act as CCN are partially water-soluble species with moderate

hygroscopicity, (~0.3) [24]. However, the CCN activity of insoluble organic material is less understood.

Meat and fatty foods cooking are major sources of cholesterol. Cholesterol can be emitted at a rate of ~7.1 $\frac{mg}{kg}$ meat when frying meat and ~72.7 $\frac{mg}{kg}$ meat when charbroiling [6]. These emissions can be less than submicrometer sizes [5].

Recent studies of cooking emissions have shown that the aerosols are hydrophobic and do not readily form droplets [36]. Direct ambient measurements suggest that the contribution of cooking aerosol in urban China increases CCN number and critical diameters in CCN Closure studies [37].

Raymond and Pandis measured CCN activity of cholesterol and found critical electrical mobility diameters equal to 101± 20 and 48 ±8*nm* at 0.3 and 1% respectively, significantly lower than predicted values assuming complete and partial dissolution [18].

Cholesterol is an insoluble organic species found readily in the atmosphere [6] with a solubility of less than 0.002 *gram* in 100 *ml* water [18]. Although cholesterol does not easily dissolve in water, it is soluble in alcohols such as acetonitrile, isopropanol, methanol, ethanol, acetone (> than 32.5 *mg* per 100 *ml* of organic solvent) [19]. It can be assumed that addition of the volatile organic solvent to the atomized solution has negligible effects; organic solvents are more volatile than water and are likely to evaporate readily during the atomization drying process. The assumption is supported by typical reported water vapor RH less than ~10% after diffusional drying. Huff-Hartz et al found that the solvent modifies the CCN activity of four compounds [34].

The CCN measurement of cholesterol was obtained at 1% supersaturation and the critical electrical mobility diameter of cholesterol was found to be > 230*nm*. This result

was obtained from the aerosol atomized from an alcohol solution; no aerosol could be generated with pure water. Huff-Hartz also stated that large activation diameters are due to insufficient efficiency of drying the particles [34].

3.3. Factors Affecting Hygroscopicity

Morphology of aerosols is an important concept since their deviation from sphere has effects in the amount and direction of scattering light in atmosphere. Hence, shape factor is a key role determining direct and indirect effects of aerosols. Soot particles, black carbon produced from combustion are examples of non-spherical particles that are called fractals. De Carlo et al. paper focuses on characterizing particle morphology and effective density [22].

Yet, organic molecules can diffuse to the surface of a growing droplet and establish an equilibrium surface tension depression. In addition, cholesterol is known to form mixed monolayer fatty acids at the water air interface [38], [39]. Thus, Li et al observed higher CCN activity from cooking oils and attributed decreases in critical diameter to lower droplet surface tensions (~30 *dyne* cm^{-1}) [40].

Moore et al. 2008 paper has focused on determining the surface tension reduction of a sample after adding ammonium sulfate to it by relating it to CCN activity of the sample. The sample has unknown chemical composition. To measure CCN activity, they carried out SMCA and surface tension measurements were done using pendant drop method with tensiometer. The agreement between direct results and SMCA data leads to the conclusion that organic molecules are able to diffuse to the surface of a growing droplet and establish an equilibrium surface tension depression [38].

Hence, in the following sections we will study hygroscopicity of cholesterol with calculating κ with two different techniques. As you learned more about the importance of shape factor and surface tension in determining a particle hygroscopicity, we would measure them and use them to correct κ.

Chapter 4: Experimental Measurement Methods

In this chapter, we review techniques used to determine factors participating in defining hygroscopicity of cholesterol. First, we would review the two different methods used to measure κ. Later, shape factor measurement setup is introduced and how κ is corrected using shape factor. Finally, surface tension measurements are described.

4.1. Particle Generation

Aerosols were generated with a Collison type atomizer. Solute was placed in solution and the atomizer generated a mist of wet droplets. Subsequently, the droplets were heated to ~85°C and then passed through one or two driers (TSI diffusion dryer 3062-NC) to remove excess moisture. In this study, 0.03 *grams* of $(NH_4)_2SO_4$ was added to 400 *ml* of ultrapure water (< 18$M\Omega$) for instrument calibration. Similar to Huff-Hartz et al, cholesterol was added to pure water; however, particles could not be generated. Thus, insoluble organic samples were prepared by dissolving 0.004 *gram* of cholesterol (with purity of 99%) in 35 *ml* of ethanol, isopropanol and acetone. Ethanol, isopropanol, and acetone were specifically chosen to explore the effects of alcohol boiling point and cholesterol solubility. Ethanol and isopropanol have similar boiling points (78.4°C, and 82.5°C, respectively [41]). The boiling point of acetone is much lower (56.5°C, [41]). The solubility of cholesterol in ethanol and acetone is ~32.5 *mg* in 100 *ml* of solvent and 3.8 [19]. The solubility of cholesterol in isopropanol is larger and ~48.9 *mg* in 100 *ml* of solvent [42]. Subsequently, 150, 300, and 450*ml* of water were added to the 35*ml* cholesterol/alcohol mixture such that the dilute alcohol solution was 7.2%, 10.4% and 18.9% by volume. A magnetic stirrer and ultrasonic sonicator (Bransonic® Ultrasonic

Baths) facilitated the mixing of the solute, alcohol and water solution. In total there were nine different samples.

4.2. Electrical Mobility CCN Measurement

In this study, scanning mobility CCN analysis (SMCA) measured the critical electrical mobility diameter, D_{mo}, of particles generated via atomization. SMCA produces high-resolution size-resolved CCN activity and growth kinetics data [21]. Briefly described here, the experimental method couples a scanning mobility particle sizer (SMPS), condensation particle counter (CPC), and Droplet Measurement Technologies (DMT) Cloud Condensation Nuclei Counter (CCNC). The SMPS uses a differential mobility analyzer (DMA TSI 3081) to electrostatically classify particles. The DMA is operated with a 10:1 sheath to aerosol flow ratio. Electrical mobility size selection assumes that particles are spherical [43]. Particle sizes between 10 nm and 286 nm were selected every 135 seconds.

The monodisperse particle stream flow was then divided and sampled by the CPC and CCNC. Both CPC 3772 and CPC 3776 ultrafine had a sample flowrate of 0.3 *lpm*. The CPC counted the total concentration of particles (CN). The CCNC was set to different supersaturations between 0.18 and 1.87 supersaturation. The CCNC counted the number of droplets formed at a constant instrument supersaturation. s. Therefore, the CCN to CN "activation" ratio for a given electrical mobility particle size and constant s was measured with the SMCA technique. The critical diameter, D_{mo} was defined as the size where the CCN/CN ratio = 50%. The schematic of this setup is provided in Figure 4.1.

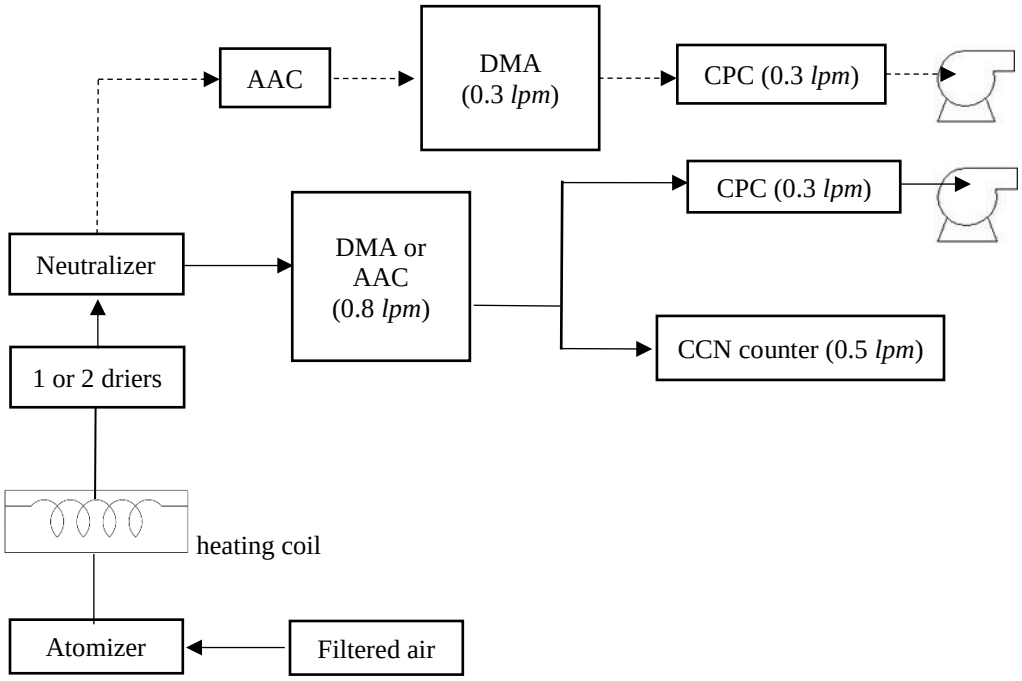

Figure 4.1. Experimental setup using DMA or AAC as a classifier. Sample flowrates are illustrated inside the parentheses. The setup shown with dashed line corresponds to the setup for shape factor.

It is worth to note that before starting SMCA, it is necessary to calibrate CCN counter with an inorganic compound which is completely soluble in water. Ammonium Sulfate with the κ value of 0.604425 was selected to calibrate supersaturations needed for experiments done further with cholesterol.

4.3. AAC CCN Measurement

SMCA produces rapid and precise critical diameters. However, the D_{mo} of non-spherical particles may overestimate the moles of dissolved solute. In a second experimental set-up, the SMPS was replaced with an aerodynamic aerosol classifier (AAC Cambustion). The AAC exploits particle settling time and size-selects the particles based on aerodynamic diameter [26]. Furthermore, no charging of particles is required in AAC measurement and there is no influence of multiply charged particles on CCN number. The

AAC aerodynamic particle selection has narrower transfer functions at larger particle sizes and is most accurate above 80*nm* [44]. Particle size was held constant at a 120*nm* aerodynamic diameter, D_{ae}. The monodisperse aerosol was then divided and sampled by the CPC and CCNC. For constant D_{ae}, the CCNC instrument supersaturations are varied from 0.18 to 1.87 with intervals of ~0.1%. Each activation ratio (CN/CCN) is plotted versus instrument *s;* it takes ~2 hours to complete one activation curve. A critical supersaturation, S_c is defined for D_{ae} at CN/CCN = 50%. Thus, $\kappa_{apparent}$ can also be calculated from aerodynamic particle measurements. D_{ae} and S_c are substituted into Equation 4 for D_d and *S*, respectively.

4.4. Shape Factor

Shape factor describes the shape of a particle, independent of its size. Both in AAC and DMA the particles are assumed to be spherical. Owing to that, it is important for us to learn about the actual shape of cholesterol particles. Shape factor is computed using Equation (22) [29].

The setup used for this set of experiments shown with dashed lines in Figure 5.3.1 is based on Tavakoli et al, 2014 method [26]. During shape factor measurements, the atomized and dried particles first move to the AAC and are selected based on aerodynamic diameter. Then, particles will go through the SMPS. D_{mo} is measured by DMA and D_{ve} is calculated using the D_{ae} set in AAC. Substituting these values into Equation (22) concludes to shape factor.

4.5. κ Values with Shape Factor Correction

As stated in Section 4.1., calculating κ when using DMA with the assumption of particles to be spherical would give us results not accurate enough. After calculating shape

factors, we can use Equations (21), (22) to calculate aerodynamic diameter from mobility diameter. Then substituting this diameter in κ equation would result in values with shape factor correction. These values are essentially comparable with the AAC κ values since they are both based on aerodynamic diameter.

4.6. Surface Tension

Surface tension is measured using a pendant drop tensiometer (Theta optical tensiometer with One Attension software). The syringe needle dispenses a drop (< 10 μL) of solution. Once the droplet has reached equilibrium, the camera captures 61 images at a rate of 0.6 frames per second. The droplet surface is fit to Young- Laplace Equation and $\sigma_{\frac{s}{a}}$ is calculated at room temperature [45]. The instrument is calibrated with ultrapure water (< 18$M\Omega$). Organic solutions are made with varying amounts of cholesterol (0, 0.004, 0.05, 0.105, 0.15, 0.2, 0.25 *grams*) added to the 7.2%, 10.4% and 18.9% (by volume) ethanol, isopropanol, and acetone dilutions. The Syskowski-Langmuir isotherm describes the depression in surface tension due to the addition of organics in solution [46]. Briefly, the fit is used to estimate surface tension at droplet activation.

Chapter 5: Hygroscopicity of Cholesterol with Respect to Various Factors

In this chapter, we cover results obtained from each set of experiments focusing on various modifying factors. Each part includes tables and graphs to help us analyze the results deeper. At the end of this chapter, we would be able to determine elements effective and compare their extent of effectiveness as well.

5.1. Electrical Mobility CCN Measurement

Figure 5.1 shows the exemplary SMCA results and activation of particles generated in 7.2%, 10.4% and 18.9% (by volume) ethanol, acetone, and isopropanol dilutions then heated and passed through one drier. A charge correction is applied to the data set and the effects of multiply charged particles are negligible.

A sigmoidal fit is applied and the D_{mo} of cholesterol from all 9 samples at 1.18% is comparable to the D_{mo} reported by Raymond and Pandis ($48 \pm 8nm$) at 1%.

It was originally assumed that the addition of alcohol would have no discernible effects on CCN activation; the alcohol and water content is evaporated through the drier during particle generation. However, as the amount of water increases the $D_{mo,}$ increases (Fig. 5.1.), thus $\kappa_{a\text{pparent}}$ decreases in all three alcohol mixtures (Table 5.1).

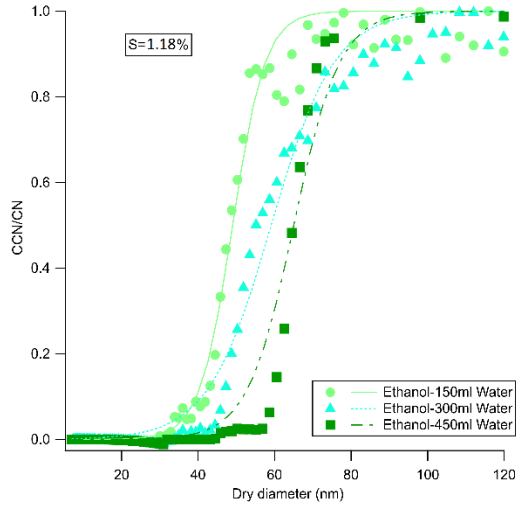

a)

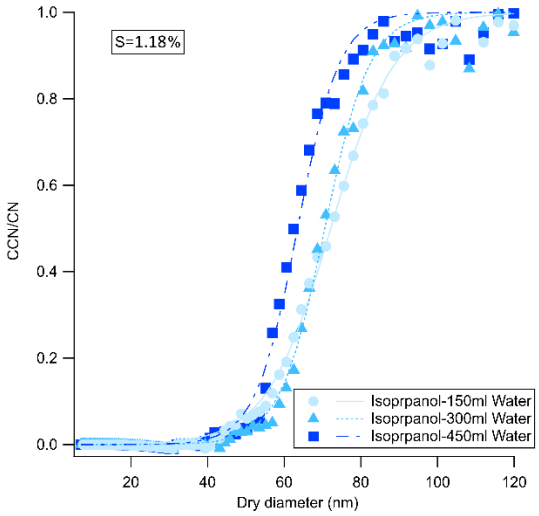

b)

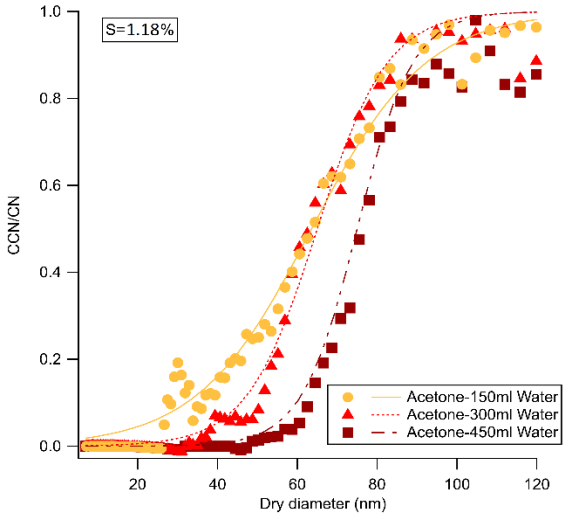

c)

Figure 5.1. CCN/CN versus Electrical mobility dry diameter (D_{mo}) at supersaturation = 1.18%. Activation curves of three samples of a) Ethanol; b) Isopropanol and c) Acetone using one drier

Average κ values can be found in Table 5.1. $\kappa_{apparent}$ for all three alcohols approaches the theoretical value for cholesterol ($\kappa_{theoretical}$) calculated from Equation (19) and cholesterol physical properties which lead to the value equal to 0.049050. It is known that solubility of cholesterol in isopropanol is the highest among the three solvents selected. Results show that solubility has influenced κ value in reaching the ultimate value faster and in higher percentage of alcohols. Cholesterol is proved to have the same solubility in acetone and ethanol while we can observe the κ values are slightly difference. This may be due to difference in boiling point which is greater for ethanol. As mentioned before in the figures, increasing the amount of water results in higher activation diameter. This can be observed in κ values as well. From κ equation we know that dry diameter and κ value are reversely proportional to each other. Thereby, increasing the amount of water will lead to higher diameter and so lower κ values.

Table 5.1. Electrical mobility κ values using SMCA utilizing one drier, the number in the parenthesis next to solvent compound indicates number of experiments run

One drier			
Solvent **Volume percentage of alcohol**	**150*ml* Water** **18.9%**	**300*ml* Water** **10.4%**	**450*ml* Water** **7.2%**
Ethanol (12)	0.087±0.022	0.0070±0.011	0.048±0.015
Isopropanol (16)	0.053±0.016	0.045±0.023	0.046±0.003
Acetone (17)	0.075±0.041	0.052±0.023	0.045±0.008

Figure 5.2 indicates the same graphs for experiments with a drier added to the previous setup. Results show that adding the drier does not affect the activation ratio trend among different samples. Thus, the same SMCA experiments were subsequently repeated with 2 diffusional driers in parallel before size selection. Results are presented in Table 5.1. $\kappa_{apparent}$ obtained after two driers are lower than with one drier. The overall average $\kappa_{apparent}$ from two driers =0.046 ± 0.013 and is similar to $\kappa_{theoretical}$ = 0.049.

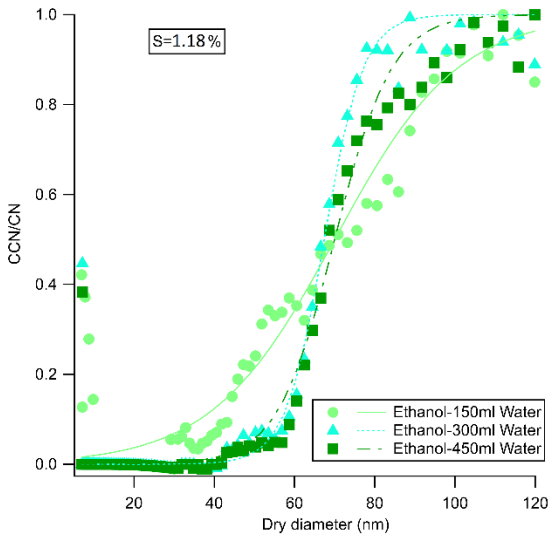

a)

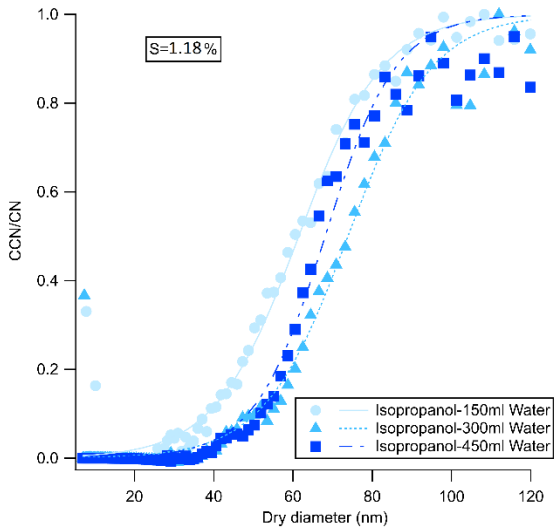

b)

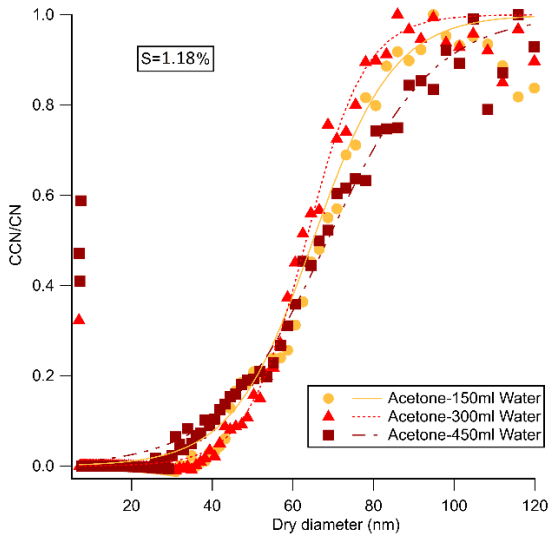

Figure 5.2. CCN/CN versus Electrical mobility dry diameter (D_{mo}) at supersaturation = 1.18%. Activation curves of three samples of a) Ethanol; b) Isopropanol and c) Acetone using two driers

c)

Table 5.2. Electrical mobility κ values using SMCA utilizing two driers, the number in the parenthesis indicates number of experiments run

Two driers			
Solvent **Volume percentage of alcohol**	**150*ml* Water** **18.9%**	**300*ml* Water** **10.4%**	**450*ml* Water** **7.2%**
Ethanol (15)	0.078±0.048	0.034±0.004	0.039±0.007
Isopropanol (28)	0.051±0.021	0.037±0.008	0.035±0.003
Acetone (17)	0.048±0.012	0.042±0.008	0.054±0.025

ANOVA statistics presented in supplementary material, Table A1 indicates that in experiments the addition of water strongly modifies the CCN activity and $\kappa_{apparent}$ (p-value = 2.99E-12 and < 5%). The type of alcohol used to generate particles also modifies CCN activity (p-value = 0.011). Specifically, the CCN activity of ethanol and acetone generated particles had a more discernible effect than those generated from isopropanol (Table 5.1-5.2). For example, at 18.9% alcohol dilutions, cholesterol generated from

isopropanol had the highest critical diameter, and lowest $\kappa_{apparent}$ (Table 5.1-5.2). The difference with isopropanol in one-drier experiments suggests that solubility of cholesterol in the specific alcohol affects measurements.

5.2. AAC CCN Measurement

Figure 5.3 shows the activation ratios of *120 nm* aerodynamic particles exposed to varying supersaturation with one drier and 5.4 using two driers. κ values were calculated from the aerodynamic critical diameter, D_{ae} (Table 5.3-5.4). The results for $\kappa_{apparent}$ from one and two driers are presented in Table 5.3-5.4. The influence of changing the volume of water in the samples can be clearly observed in one drier data but not in two driers. Both the volume of water and number of driers used are significant factors in the $\kappa_{apparent}$ response. In other words, for both SMCA and AAC measurements, diluting the alcohol in the solution reduces the influence of the organic solvents. Thus, the following experiments explore the effects of alcohol solutions for the most important κ-Köhler theory activation assumptions, constant surface tension and spherical shape factor.

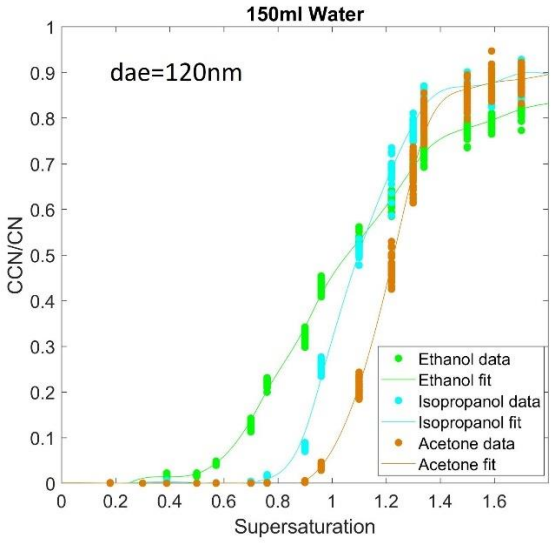

a)

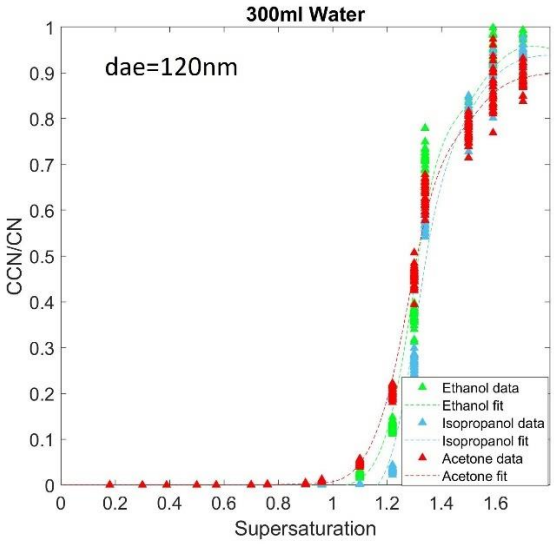

b)

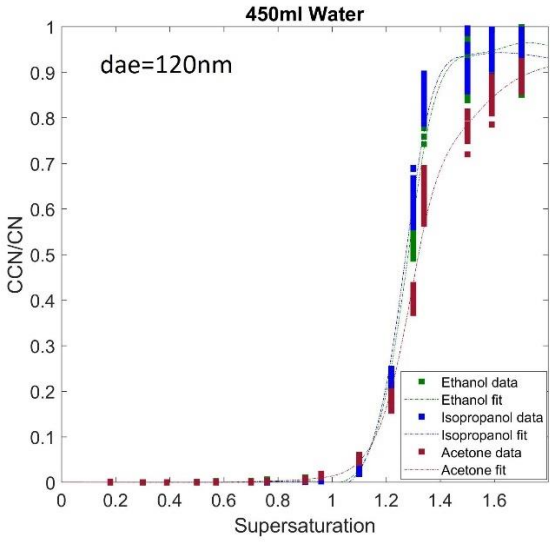

c)

Figure 5.3. Activation ratio versus supersaturation for all three solvents mixed with a) 150ml, b) 300ml and c) 450ml water using one drier

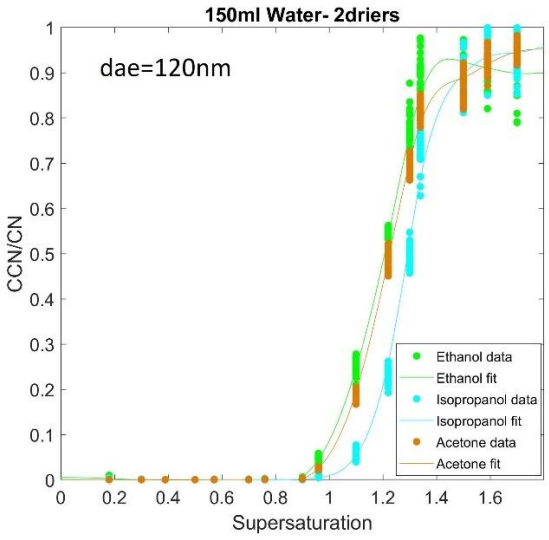

a)

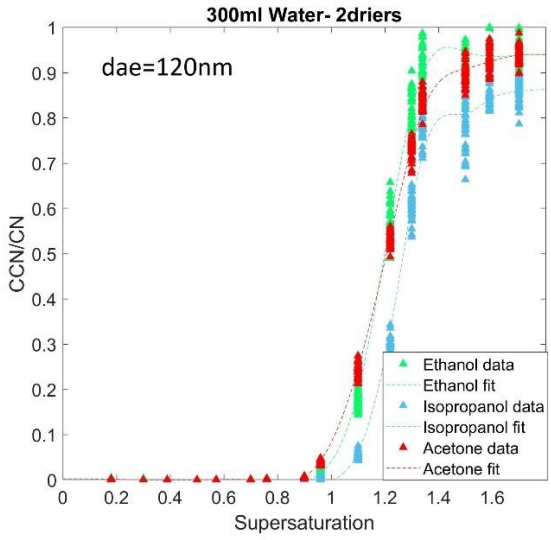

b)

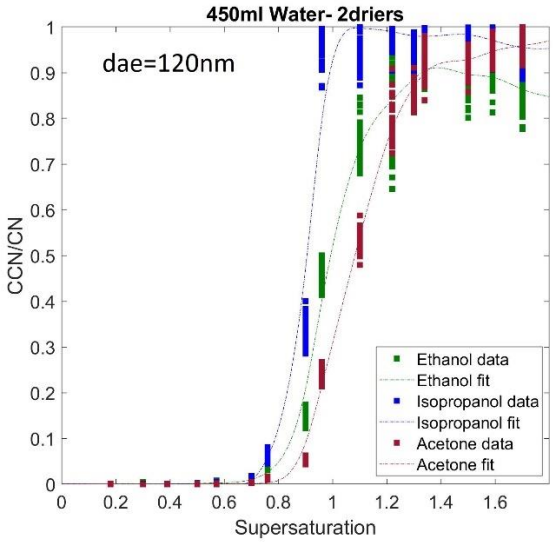

c)

Figure 5.4. Activation ratio versus supersaturation for all three solvents mixed with a) 150ml; b) 300ml and c) 450ml water using two driers

Table 5.3. AAC κ values using one drier

One drier			
Solvent **Volume percentage of alcohol**	**150*ml* Water** **18.9%**	**300*ml* Water** **10.4%**	**450*ml* Water** **7.2%**
Ethanol	0.0064	0.0045	0.0049
Isopropanol	0.0056	0.0042	0.0050
Acetone	0.0047	0.0045	0.0044

Table 5.4. AAC κ values using two driers

Two driers			
Solvent **Volume percentage of alcohol**	**150*ml* Water** **18.9%**	**300*ml* Water** **10.4%**	**450*ml* Water** **7.2%**
Ethanol	0.0076	0.0089	0.0076
Isopropanol	0.0062	0.0067	0.0091
Acetone	0.0055	0.0055	0.0067

We observe a difference in two orders of magnitude between electrical mobility derived κ and AAC derived κ values. $(NH_4)_2SO_4$ calibrations using AAC and SMCA produce consistent critical D_{mo} and D_{ae} and similar κ values (see, supplementary material).

As mentioned before AAC works best in sizes larger than 80*nm* [44]. That is why we would not be able to obtain a good curve and correct κ when running the experiment in diameters lower than 80*nm*.

ANOVA analysis for AAC κ values implies that number of driers used in the experiment is more effective in changing κ rather than water volume.

5.3. Shape Factor

It is measured that the average shape factor of cholesterol is equal to 1; which means the particles are almost spherical. In addition, effective density equals density of cholesterol at shape factor 1. However, as you can see in the larger diameters, shape factor goes lower than 1. This is because particles with larger diameters do not stick to each other, cannot maintain the compact structure and so act more chain-like [31] and in lower diameters the shape factor is larger than one which means particles are more like aggregates and fractals [22].

Results from Figures 5.5, 5.6 show that sample with 150*ml* water which has the lowest amount of water, seems to act more spherical in the whole range of diameters but as we move to greater volumes of water, the chain-like effect is more significant. Also, increasing the water amount leads to higher difference between highest and lowest shape factor especially in the diameter range we operate SMCA.

Adding one drier leads to less chain-like effect in greater diameters and increases discrepancy between maximum and minimum. Results show greater separation in two driers graphs which is related to more effective removal of water. The more removal causes drier particles and so less spherical particles which can be approved by the graphs. If you consider data at a given diameter, shape factor for particles are greater when using two driers. Furthermore, it can be derived that shape factor decreases by reducing the percentage of alcohol and this can be observed more obviously in two driers graphs.

Also, it is perceived that the descending trend of cholesterol's shape factor is similar to sodium chloride studied in Biskos et al, 2006 [47].

Performing ANOVA for both 100*nm* (as an example of low diameter) and 250*nm* (as an example of high diameter) leads to the conclusion that number of driers utilized is the modifying factor in low diameters and water volume can be the determinative factor in higher diameters.

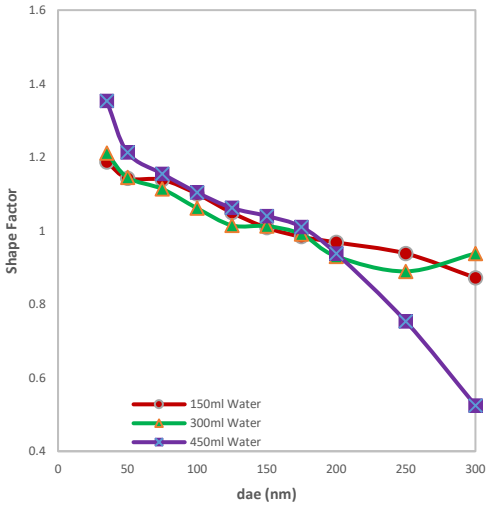

a)

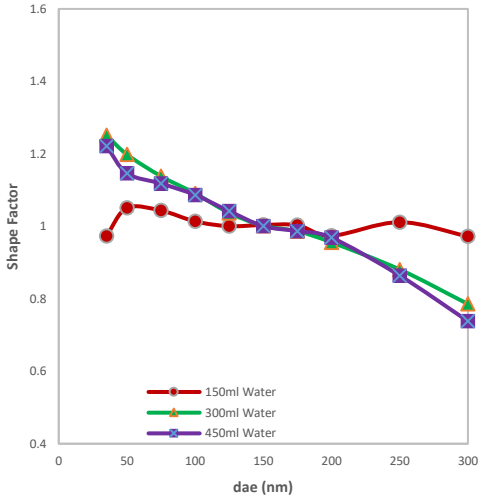

b)

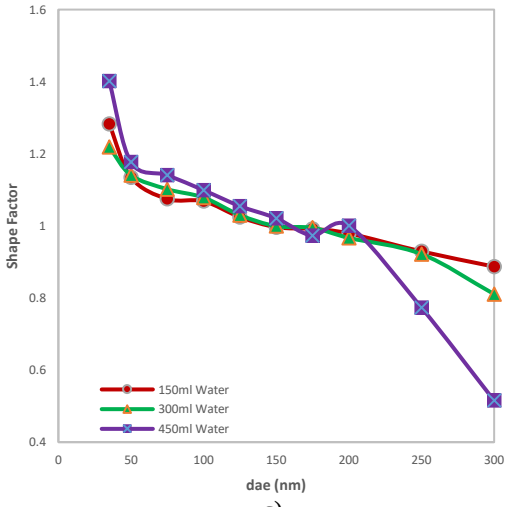

c)

Figure 5.5. a) Ethanol; b) Isopropanol; c) Acetone shape factor for the three samples using one drier

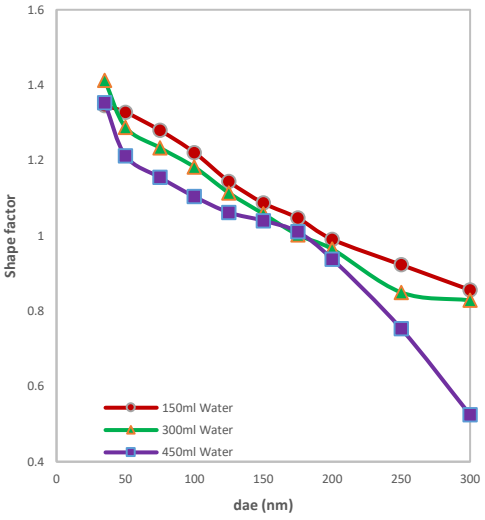

a)

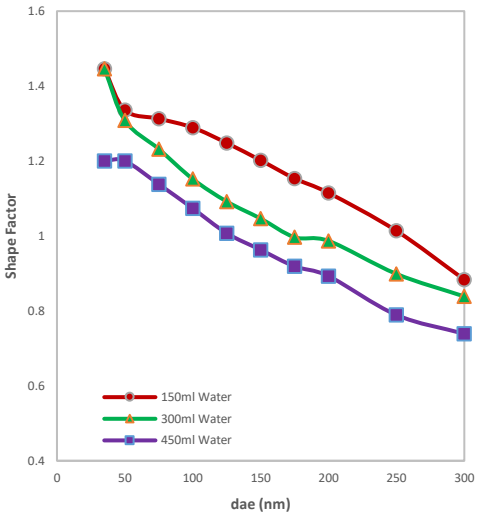

b)

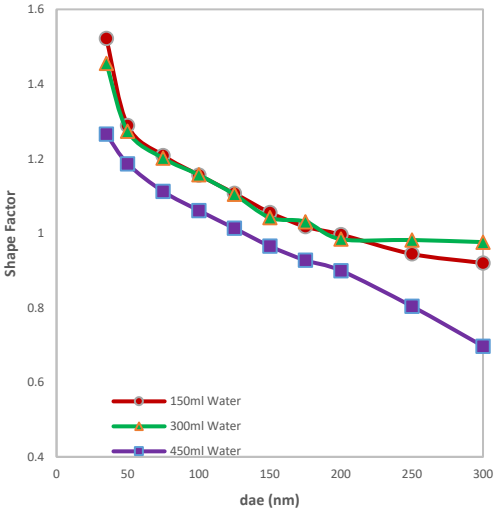

c)

Figure 5.6. a) Ethanol; b) Isopropanol; c) Acetone shape factor for the three samples using two driers

5.4. *κ Values with Shape Factor Correction*

Table 5.5 includes κ values after applying shape factor correction. It is implied that the trend is almost the same as the κ values without correction. However, a noticeable point is about samples containing 450*ml* water. This set of samples surprisingly have greater values compared to 300*ml* water samples. This is due to the shape factor described in previous section that had the largest impact on samples with large amount of water

specifically in lower diameters that SMCA is performed. In fact, in this range the shape factor for 450*ml* samples is significantly greater than 300*ml* samples while this is reverse for two driers results. And this can be observed in Table 5.6 where κ values for 450*ml* samples are not larger.

Table 5.5. Electrical mobility κ values using SMCA with shape factor correction when using one drier, the number in the parenthesis next to solvent compound indicates number of experiments run

One drier			
Solvent **Volume percentage of alcohol**	**150*ml* Water** **18.9%**	**300*ml* Water** **10.4%**	**450*ml* Water** **7.2%**
Ethanol (12)	0.103±0.029	0.0084±0.022	0.091±0.047
Isopropanol (16)	0.061±0.006	0.051±0.027	0.053±0.013
Acetone (17)	0.117±0.087	0.061±0.032	0.090±0.042

Table 5.6. Electrical mobility κ values using SMCA with shape factor correction when using two driers, the number in the parenthesis next to solvent compound indicates number of experiments run

Two driers			
Solvent **Volume percentage of alcohol**	**150*ml* Water** **18.9%**	**300*ml* Water** **10.4%**	**450*ml* Water** **7.2%**
Ethanol (15)	0.164±0.102	0.076±0.024	0.097±0.037
Isopropanol (28)	0.143±0.075	0.095±0.043	0.042±0.006
Acetone (17)	0.171±0.055	0.132±0.064	0.073±0.050

ANOVA is performed for κ values with shape factor correction illustrates that ratio of water volume to alcohol is the main factor impacting results. Hence, the conclusions made based on results from both ANOVA analyses are almost the same although values are quantitatively different.

5.5. Surface Tension

Surface tension of various concentrations of cholesterol in each sample is measured. The results are plotted in Figure 5.7. It can be understood from the graph that surface tension is changing where κ does. Surface tension is increasing with increase in volume of water. This is expected based on reference table from Vazquez et al. paper [48]. There is also more difference between surface tension of 150*ml* and 300*ml* samples than between 300*ml* and 450*ml* likewise their κ values. Hence, it can be derived that surface tension is an effective factor in modifying κ values.

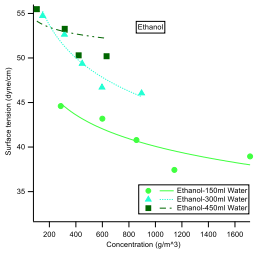

a)

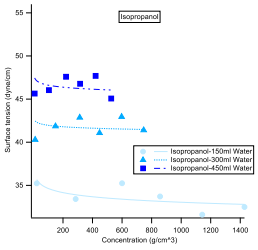

b)

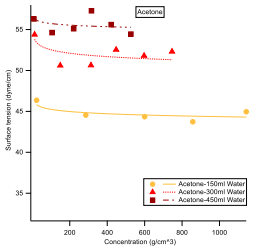

c)

Figure 5.7. Surface tension vs concentration of cholesterol in a) Ethanol; b) Isopropanol; c) Acetone mixed with three different volumes of water

Next, we assume surface tension of each mixture is the surface tension of specific volume of water and alcohol. Substituting the measured values in the κ equation instead of pure water surface tension provides us the electrical mobility κ with surface tension correction which is included in Table 5.7 for one drier and Table 5.8 for two driers data. It is observed that after applying the surface tension correction, κ values are almost constant. Thereby, surface tension is the major factor affecting κ values when using mixtures of water and alcohol with various volume ratios.

Table 5.7. Electrical mobility κ values with surface tension correction when using one drier, the number in the parenthesis next to solvent compound indicates number of experiments run

One drier			
Solvent **Volume percentage of alcohol**	**150*ml* Water** **18.9%**	**300*ml* Water** **10.4%**	**450*ml* Water** **7.2%**
Ethanol (12)	0.010±0.002	0.011±0.002	0.015±0.005
Isopropanol (16)	0.006±0.001	0.010±0.005	0.011±0.002
Acetone (17)	0.017±0.010	0.017±0.007	0.019±0.003

Table 5.8. Electrical mobility κ values with surface tension correction when using two driers, the number in the parenthesis next to solvent compound indicates number of experiments run

Two driers			
Solvent **Volume percentage of alcohol**	**150*ml* Water** **18.9%**	**300*ml* Water** **10.4%**	**450*ml* Water** **7.2%**
Ethanol (15)	0.011±0.003	0.013±0.002	0.023±0.002
Isopropanol (28)	0.010±0.006	0.006±0.001	0.012±0.002
Acetone (17)	0.005±0.002	0.008±0.002	0.008±0.001

Also, we would apply the same surface tension correction to AAC κ values. Results are shown in Table 5.9 for one drier experiment and Table 5.10 for two driers experiment.

Table 5.9. AAC κ values with surface tension correction when using one drier

One drier			
Solvent **Volume percentage of alcohol**	**150*ml* Water** **18.9%**	**300*ml* Water** **10.4%**	**450*ml* Water** **7.2%**
Ethanol	0.00087	0.00081	0.00163
Isopropanol	0.00066	0.00089	0.00117
Acetone	0.00128	0.00148	0.00196

Table 5.10. AAC κ values with surface tension correction when using two driers

Two driers			
Solvent **Volume percentage of alcohol**	**150*ml* Water** **18.9%**	**300*ml* Water** **10.4%**	**450*ml* Water** **7.2%**
Ethanol	0.00075	0.00089	0.00271
Isopropanol	0.00051	0.00112	0.00219
Acetone	0.00130	0.00181	0.00296

The results obtained from applying surface tension correction factor to electrical mobility κ, are not comparable to the AAC κ. To make this happen, we need electrical mobility κ values with both shape factor and surface tension correction. Table 5.11 illustrates the values when only one drier was used, and Table 5.12 corresponds to corrected values when adding a drier. The average is ~0.028±0.02. It is observed that after applying all the correction, the trend is the same for both AAC κ and electrical mobility κ although they still have that order of magnitude difference. The hygroscopicity of particle is increasing as the amount of alcohol in the dilution is reduced for all the samples. This is explained well by surface tension increase and also shape factor changes.

Table 5.11. Electrical mobility κ values with shape factor and surface tension correction when using one drier, the number in the parenthesis next to solvent compound indicates number of experiments run

One drier			
Solvent **Volume percentage of alcohol**	**150*ml* Water** **18.9%**	**300*ml* Water** **10.4%**	**450*ml* Water** **7.2%**
Ethanol (12)	0.013±0.003	0.014±0.003	0.029±0.015
Isopropanol (16)	0.007±0.001	0.011±0.006	0.013±0.003
Acetone (17)	0.027±0.021	0.020±0.011	0.039±0.019

Table 5.12. Electrical mobility κ values with shape factor and surface tension correction when using two driers, the number in the parenthesis next to solvent compound indicates number of experiments run

Two driers			
Solvent **Volume percentage of alcohol**	**150*ml* Water** **18.9%**	**300*ml* Water** **10.4%**	**450*ml* Water** **7.2%**
Ethanol (15)	0.021±0.013	0.013±0.004	0.031±0.012
Isopropanol (28)	0.015±0.008	0.020±0.009	0.010±0.001
Acetone (17)	0.041±0.013	0.036±0.019	0.032±0.022

ANOVA analysis for corrected electrical mobility κ leads to the consequence that solvent is the modifying factor. However, corrected AAC κ leads to the conclusion that amount of water is still the modifying factor. The reason is that the alcohol and the amount of water added have interactions. In the cases where shape factor is accounted for, the interaction should be negligible. Furthermore, we know that the depending on the dilution concentration we can obtain more/less spherical particles. In the cases where shape factor is not specifically accounted for, (AAC measurements) the interactions of alcohol and water volume are likely to have an impact. Thus, after shape factor and surface tension corrections are applied to electrical mobility the type of alcohol used to generate fractal particles modifies κ. For the corrected AAC measurements, surface tension has been accounted for, but the impact of changing shape has not. Fractal particles have more surface area than spherical particles, and thus more potential sites for water vapor condensation.

Chapter 6: Conclusion

In the present study, we studied hygroscopicity of dissolving cholesterol in mixtures of water and distinct alcohols as solvents. Samples consist of various amounts of water added to ethanol, isopropanol and acetone. To determine hygroscopicity, κ was calculated for all samples and results showed that the presence of a small amount of organic solvents, such as alcohol can promote droplet formation. The first method run to calculate κ was SMCA. Later, to avoid impacts of applied charges in DMA, the classifier was replaced with an AAC to measure κ with a different technique. Two orders of magnitude difference can be observed between κ values found from the two different methods while the trend is almost the same. The difference can be because of water or alcohol trapped in porous fractals when running measurements that make diffusion happen less efficient and lead to higher hygroscopicity in compare to using aerodynamic diameter with AAC.

Moreover, shape factor of cholesterol was measured to determine whether it is influencing the size selection or not. Then, we used the shape factor of cholesterol to correct κ values obtained using DMA. Analysis of variance was performed both for κ values without and with shape factor correction. Results of the analyses indicated that the amount of water mixed with alcohol is modifying κ results and that shape factor cannot explain the change. By looking through papers, it could be learned that boiling point is not playing an important role since it is almost constant when percentage of alcohol is changing [49]. Further, surface tension measurements strongly agreed with previous studies. It has been proved that existence of organics would decrease surface tension. It is at droplet sizes and solute concentrations below and close to critical size that surface

tension most effectively influences whether a droplet form [21]. As expected, surface tension of water and alcohol mixture is lower than pure water and, also increasing the amount of cholesterol dissolved in the solution leads to reduction in surface tension. The higher amount of water in sample results in larger surface tension. Substituting new surface tension values in the electrical mobility κ equation provides us an almost constant value. Therefore, it can be deduced that surface tension is playing the main role in changing hygroscopicity of cholesterol and so the κ values. Besides, we can compare electrical mobility κ which has shape factor and surface tension correction with surface tension corrected AAC κ. The trend is the same for both. As we increase amount of water in the dilution, the ability of particles to form droplet increases. The κ values we get for electrical mobility κ and AAC κ are almost within the range of values obtained in previous studies. Li et al found the κ value of 0.08 for fresh particles and 0.14 for aged aerosols [40]. Shiling et al conducted the research for oleic acid which led to κ equal to 0.008 [36]. Raymond and Pandis repeated the experiment for cholesterol at supersaturation 0.3% and 1% with κ 0.15 and 0.13 [18]. Also, Huff-Hartz et al have done the study for cholesterol dissolved in alcohol using two driers. They concluded the κ value of smaller than 0.0011 at supersaturation 1% [34].

6.1. Future Work

Useful information was obtained from the results found in this study which create the need for future work. Performing these experiments for other insoluble compounds which are dissolvable in alcohols should be done. Further studies on surface tension of organics and the effects on hygroscopicity if of desire. Also, there should be more studies concerning hygroscopicity of particles dissolved in different solvents other than water.

Appendices

ANOVA (Analysis of variance)

As seen up to this point, there are mainly two factors influencing the κ value:

- Solvent used
- Volume of water consumed to make samples

To determine which one is the most effective, analysis of variance (ANOVA) is performed using Excel software. Table A.9 is indicating the result of ANOVA done for electrical mobility κ values without shape factor correction. P-value is set at 5%. As you can see, P-value for both factors are less than 5% which leads us to the conclusion that null hypothesis is rejected and they both are modifying factors. Although, more precision alert us that this value for the amount of water factor is considerably lower than the significant value of 5% in comparison to the solvent factor. The P-value for interaction is lower than 5%, too. However, it is not as significant as amount of water. Thereby, we would neglect it.

The same data analysis is performed for electrical mobility κ values after shape factor correction is applied in Table A.10. The conclusions we get are the same as before. Besides, it is worth pointing out that the degree of freedom for both analyses is 242 which makes it unnecessary to include probability plot.

Table A.9. Detailed analysis of variance between solvent and amount of water without considering shape factor correction

ANOVA

Source of Variation	*SS*	*df*	*MS*	*F*	*P-value*	*F crit*
Sample	0.005661	2	0.00283	4.56187	0.011388	3.034414
Columns	0.036963	2	0.018482	29.78683	2.99E-12	3.034414
Interaction	0.007269	4	0.001817	2.928886	0.021665	2.410222
Within	0.145188	234	0.00062			
Total	0.195081	242				

Table A.10. Detailed analysis of variance between solvent and amount of water considering shape factor correction

ANOVA

Source of Variation	*SS*	*df*	*MS*	*F*	*P-value*	*F crit*
Solvent	0.041993	2	0.020996	5.760468	0.003613242	3.034414
Amount of water	0.243956	2	0.121978	33.46535	1.65072E-13	3.034414
Interaction	0.007948	4	0.001987	0.545167	0.702725397	2.410222
Within	0.852909	234	0.003645			
Total	1.146807	242				

The analysis is also performed for AAC κ and shape factor results to figure out what is the major factor affecting them. The ANOVA results for AAC κ in Table A.11-A.13 show the number of driers is most effective.

Table A.11. Detailed analysis of variance between solvent and amount of water for AAC κ values

ANOVA

Source of Variation	*SS*	*df*	*MS*	*F*	*P-value*	*F crit*
Solvent	6.32E-06	2	3.16E-06	0.998886	0.405714	4.256494729
Water volume	9.47E-07	2	4.73E-07	0.149668	0.863093	4.256494729
Interaction	2.63E-06	4	6.57E-07	0.207823	0.927642	3.633088511
Within	2.85E-05	9	3.16E-06			
Total	3.84E-05	17				

Table A.12. Detailed analysis of variance between solvent and number of driers for AAC κ values

ANOVA

Source of Variation	*SS*	*df*	*MS*	*F*	*P-value*	*F crit*
Solvent	6.32E-06	2	3.15895E-06	3.857701	0.050846	3.885294
No. of driers	2.06E-05	1	2.06317E-05	25.1954	0.000299	4.747225
Interaction	1.58E-06	2	7.89854E-07	0.964567	0.40883	3.885294
Within	9.83E-06	12	8.1887E-07			
Total	3.84E-05	17				

Table A.13. Detailed analysis of variance between number of driers and amount of water for AAC κ values

ANOVA

Source of Variation	*SS*	*df*	*MS*	*F*	*P-value*	*F crit*
Volume of Water	9.47E-07	2	4.73E-07	0.442232	0.652664	3.885294
No. of driers	2.06E-05	1	2.06E-05	19.27655	0.00088	4.747225
Interaction	3.93E-06	2	1.97E-06	1.837694	0.201269	3.885294
Within	1.28E-05	12	1.07E-06			
Total	3.84E-05	17				

Analysis of variance for shape factor results is performed in two different diameters: 100*nm* as an example of low sizes and 250*nm* for large sizes. From Table A.14-A.19, it can be derived that number of driers is the modifying factor for low diameters and volume of water for high diameters.

Table A.14. Detailed analysis of variance between solvent and amount of water for shape factor results at 100*nm*

ANOVA

Source of Variation	*SS*	*df*	*MS*	*F*	*P-value*	*F crit*
Solvent	0.001312	2	0.000656	0.098272	0.907361	4.256495
Amount of Water	0.009613	2	0.004807	0.720012	0.512784	4.256495
Interaction	0.001674	4	0.000418	0.062684	0.991469	3.633089
Within	0.060083	9	0.006676			
Total	0.072682	17				

Table A.15. Detailed analysis of variance between solvent and amount of water for shape factor results at 250*nm*

ANOVA

Source of Variation	*SS*	*df*	*MS*	*F*	*P-value*	*F crit*
Solvent	71515.07	2	35757.54	1.000102	0.40531	4.256495
Amount of Water	71352.04	2	35676.02	0.997822	0.406067	4.256495
Interaction	142989.8	4	35747.44	0.99982	0.45587	3.633089
Within	321784.9	9	35753.88			
Total	607641.8	17				

Table A.16. Detailed analysis of variance between solvent and number of driers for shape factor results at 100*nm*

ANOVA

Source of Variation	*SS*	*df*	*MS*	*F*	*P-value*	*F crit*
Solvent	0.001312	2	0.000656	0.186515	0.832207	3.885294
Number of driers	0.024642	1	0.024642	7.005654	0.021304	4.747225
Interaction	0.004519	2	0.00226	0.64237	0.543212	3.885294
Within	0.042209	12	0.003517			
Total	0.072682	17				

Table A.17. Detailed analysis of variance between solvent and number of driers for shape factor results at 250*nm*

ANOVA

Source of Variation	*SS*	*df*	*MS*	*F*	*P-value*	*F crit*
Solvent	0.010096	2	0.005048	0.577351	0.576237	3.885294
Number of driers	2.22E-05	1	2.22E-05	0.002542	0.960622	4.747225
Interaction	0.002901	2	0.001451	0.165917	0.849027	3.885294
Within	0.104924	12	0.008744			
Total	0.117944	17				

Table A.18. Detailed analysis of variance between amount of water and number of driers for shape factor results at 100*nm*

ANOVA

Source of Variation	*SS*	*df*	*MS*	*F*	*P-value*	*F crit*
Amount of water	0.009613	2	0.004807	3.703176	0.055902	3.885294
Number of driers	0.024642	1	0.024642	18.98459	0.000933	4.747225
Interaction	0.022851	2	0.011426	8.802388	0.004435	3.885294
Within	0.015576	12	0.001298			
Total	0.072682	17				

Table A.19. Detailed analysis of variance between amount of water and number of driers for shape factor results at 250*nm*

ANOVA

Source of Variation	*SS*	*df*	*MS*	*F*	*P-value*	*F crit*
Amount of water	0.088937333	2	0.044468667	18.93537	0.000194	3.885294
Number of driers	2.22222E-05	1	2.22222E-05	0.009463	0.924113	4.747225
Interaction	0.000803111	2	0.000401556	0.170988	0.844849	3.885294
Within	0.028181333	12	0.002348444			
Total	0.117944	17				

Further, Table A.20- A.22 provides the analysis of variance for κ after surface tension and shape factor correction is applied. At the end, Table A.23 is the analysis of variance for surface tension values which shows amount of water is a stronger factor.

Table A.20. Detailed analysis of variance between solvent and amount of water for electrical mobility κ after surface tension and shape factor correction.

ANOVA

Source of Variation	*SS*	*df*	*MS*	*F*	*P-value*	*F crit*
Solvent	832.4234	2	416.2117	93.16911	5.85E-15	3.259446
Amount of water	1119.856	2	559.9282	125.3401	6.03E-17	3.259446
Interaction	7.867929	4	1.966982	0.44031	0.778616	2.633532
Within	160.8218	36	4.467271			
Total	2120.97	44				

ANOVA

Source of Variation	*SS*	*df*	*MS*	*F*	*P-value*	*F crit*
Solvent	0.001203	2	0.000602	14.95994	0.001375	4.256495
Amount of water	0.000144	2	7.22E-05	1.79558	0.220696	4.256495
Interaction	0.000245	4	6.13E-05	1.524171	0.274762	3.633089
Within	0.000362	9	4.02E-05			
Total	0.001955	17				

Table A.21. Detailed analysis of variance between solvent and number of driers for electrical mobility κ after surface tension and shape factor correction.

ANOVA

Source of Variation	*SS*	*df*	*MS*	*F*	*P-value*	*F crit*
Solvent	0.001203	2	0.000602	11.69654	0.001519	3.885294
Number of driers	0.000118	1	0.000118	2.285097	0.156501	4.747225
Interaction	1.68E-05	2	8.39E-06	0.163067	0.851385	3.885294
Within	0.000617	12	5.14E-05			
Total	0.001955	17				

Table A.22. Detailed analysis of variance between amount of water and number of driers for electrical mobility κ after surface tension and shape factor correction.

CCN Calibration with $(NH_4)_2SO_4$:

Figure S.12 illustrates the calibrated supersaturations obtained from calibrating CCN counter with 0.03 *grams* of $(NH_4)_2SO_4$ in 300*ml* H_2O. The setup operated is the one indicated in Figure S.2 with DMA as the classifier.

Table A.23. Calibrated supersaturations used in CCN measurements

Instrument supersaturation	Calibrated supersaturation	Critical diameter (nm)
0.2	0.18	86.42
0.4	0.40±0.02	52.42±1.56
0.6	0.56±0.04	41.34±1.84
0.8	0.74±0.01	34.96±0.39
1	0.95±0.01	29.66±0.23
1.2	1.18±0.05	25.72±0.73
1.4	1.31±0.02	23.97±0.31
1.6	1.64±0.06	20.71±0.54
1.8	1.87±0.02	18.96±0.12

References

[1] Pöschl, U., n.d. Atmospheric Aerosols: Composition, Transformation, Climate and Health Effects. Angewandte Chemie International Edition 44, 7520–7540.

[2] Essiett A.A., Bede M. C. Assessment of Total Suspended Particulates (TSP) in Ikot Abasi L. G. A., Nigeria. International Journal of Physics. 2015; 3(6):230-232.
doi: 10.12691/ijp-3-6-1

[3] Schwartz, J., Dockery, D., 1992. Increased Mortality in Philadelphia Associated with Daily Air Pollution Concentrations. The American review of respiratory disease 145, 600–4.

[4] Dusek, U., Frank, G.P., Curtius, J., Drewnick, F., Schneider, J., Kürten, A., Rose, D., Andreae, M.O., Borrmann, S., Pöschl, U., 2010. Enhanced organic mass fraction and decreased hygroscopicity of cloud condensation nuclei (CCN) during new particle formation events.
Geophysical Research Letters 37. https://doi.org/10.1029/2009GL040930

[5] Hildemann, L.M., Markowski, G.R., Jones, M.C., Cass, G.R., 1991. Submicrometer Aerosol Mass Distributions of Emissions from Boilers, Fireplaces, Automobiles, Diesel Trucks, and Meat-Cooking Operations. Aerosol Science and Technology 14, 138–152. https://doi.org/10.1080/02786829108959478

[6] Rogge, W.F., Hildemann, L.M., Mazurek, M.A., Cass, G.R., Simoneit, B.R.T., 1991. Sources of fine organic aerosol. 1. Charbroilers and meat cooking operations. Environmental Science & Technology 25, 1112–1125.

[7] “Cloud Climatology: The Role of Clouds in Climate”
URL: https://isccp.giss.nasa.gov/role.html#ROLE

[8] “Cloud Climatology: System of Climate Feedbacks Involving Clouds”
URL: https://isccp.giss.nasa.gov/role.html#ROLE

[9] Fennelly, P.F., 1976. The Origin and Influence of Airborne Particulates: Both man-made and natural processes contribute to the concentration of particulate matter in the atmosphere; the effects of this aerosol on human health, environment, and climate are just beginning to be understood. American Scientist 64, 46–56.

[10] Tomasi, C., Lupi, A., 2016. Primary and Secondary Sources of Atmospheric Aerosol, in: Tomasi, C., Fuzzi, S., Kokhanovsky, A. (Eds.), Atmospheric Aerosols. Wiley-VCH Verlag GmbH & Co. KGaA, Weinheim, Germany, pp. 1–86. https://doi.org/10.1002/9783527336449.ch1

[11] "6 VOCs and NOx: Relationship to Ozone and Associated Pollutants." National Research Council. 1991. Rethinking the Ozone Problem in Urban and Regional Air Pollution. Washington, DC: The National Academies Press. doi: 10.17226/1889.

[12] Seinfeld, J.H., Pandis, S.N., 1998. Chemistry of the atmospheric aqueous phase. Atmospheric Chemistry and Physics: From Air Pollution to Climate Change 337407.

[13] IPCC, 2013: Summary for Policymakers. In: Climate Change 2013: The Physical Science Basis. Contribution of Working Group I to the Fifth Assessment Report of the Intergovernmental Panel on Climate Change [Stocker, T.F., D. Qin, G.-K. Plattner, M. Tignor, S.K. Allen, J. Boschung, A. Nauels, Y. Xia, V. Bex and P.M. Midgley (eds.)]. Cambridge University Press, Cambridge, United Kingdom and New York, NY, USA.

[14] US EPA, O., 2014. Criteria Air Pollutants [WWW Document]. US EPA. URL https://www.epa.gov/criteria-air-pollutants

[15] Löndahl, J., Möller, W., Pagels, J.H., Kreyling, W.G., Swietlicki, E., Schmid, O., 2014. Measurement Techniques for Respiratory Tract Deposition of Airborne Nanoparticles: A Critical Review. J Aerosol Med Pulm Drug Deliv 27, 229–254. https://doi.org/10.1089/jamp.2013.1044

[16] Bernstein, J.A., Alexis, N., Barnes, C., Bernstein, I.L., Nel, A., Peden, D., Diaz-Sanchez, D., Tarlo, S.M., Williams, P.B., Bernstein, J.A., 2004. Health effects of air pollution. Journal of Allergy and Clinical Immunology 114, 1116–1123. https://doi.org/10.1016/j.jaci.2004.08.030)

[17] National Center for Biotechnology Information. PubChem Compound Database; CID=5997, https://pubchem.ncbi.nlm.nih.gov/compound/5997

[18] Raymond, T.M., Pandis, S.N., n.d. Cloud activation of single-component organic aerosol particles. Journal of Geophysical Research: Atmospheres 107, AAC 16-1-AAC 16-8. https://doi.org/10.1029/2002JD002159

[19] Bar, L.K., Garti, N., Sarig, S., Bar, R., 1984. Solubilities of cholesterol, sitosterol, and cholesteryl acetate in polar organic solvents. Journal of Chemical & Engineering Data 29, 440–443.

[20] Kanakidou, M., Seinfeld, J.H., Pandis, S.N., Barnes, I., Dentener, F.J., Facchini, M.C., Dingenen, R.V., Ervens, B., Nenes, A., Nielsen, C.J., Swietlicki, E., Putaud, J.P., Balkanski, Y., Fuzzi, S., Horth, J., Moortgat, G.K., Winterhalter, R., Myhre, C.E.L., Tsigaridis, K., Vignati, E., Stephanou, E.G., Wilson, J., 2005. Organic aerosol and global climate modelling: a review. Atmos. Chem. Phys. 71.

[21] Facchini, M.C., Mircea, M., Fuzzi, S., Charlson, R.J., 1999. Cloud albedo enhancement by surface-active organic solutes in growing droplets. Nature 401, 257–259. https://doi.org/10.1038/45758

[22] DeCarlo, P.F., Slowik, J.G., Worsnop, D.R., Davidovits, P., Jimenez, J.L., 2004. Particle Morphology and Density Characterization by Combined Mobility and Aerodynamic Diameter Measurements. Part 1: Theory. Aerosol Science and Technology 38, 1185–1205. https://doi.org/10.1080/027868290903907

[23] Seinfeld, J.H., Pandis, S.N., 2006. Atmospheric chemistry and physics: from air pollution to climate change, 2nd ed. ed. J. Wiley, Hoboken, N.J.

[24] Petters, M. D. and Kreidenweis, S. M.: A single parameter representation of hygroscopic growth and cloud condensation nucleus activity, Atmos. Chem. Phys., 7, 1961-1971, doi:10.5194/acp-7-1961-2007, 2007.

[25] Moore, R.H., Nenes, A., Medina, J., 2010. Scanning Mobility CCN Analysis—A Method for Fast Measurements of Size-Resolved CCN Distributions and Activation Kinetics. Aerosol Science and Technology 44, 861–871.

[26] Tavakoli, F., Olfert, J.S., 2014. Determination of particle mass, effective density, mass mobility exponent, and dynamic shape factor using an aerodynamic aerosol classifier and a differential mobility analyzer in tandem. Journal of Aerosol Science 75, 35–42.

[27] Dusek, U., Frank, G.P., Curtius, J., Drewnick, F., Schneider, J., Kürten, A., Rose, D., Andreae, M.O., Borrmann, S., Pöschl, U., 2010. Enhanced organic mass fraction and decreased hygroscopicity of cloud condensation nuclei (CCN) during new particle formation events. Geophysical Research Letters 37. https://doi.org/10.1029/2009GL040930

[28] Asa-Awuku, A., Nenes, A., 2007. Effect of solute dissolution kinetics on cloud droplet formation: Extended Köhler theory. Journal of Geophysical Research: Atmospheres 112. https://doi.org/10.1029/2005JD006934

[29] P. Kulkarni, P. Baron, K. Willeke. *Aerosol Measurement principles, techniques, and applications.* 3rd edition, p.510-513: Wiley, 1992

[30] Jennings, S (1988). "The mean free path in air". Journal of Aerosol Science. **19**(2): 159. doi:10.1016/0021-8502(88)90219-4.

[31] Wolfgang Zeller (1985) Direct Measurement of Aerosol Shape Factors, Aerosol Science and Technology, 4:1, 45-63, DOI: 10.1080/02786828508959038

[32] Khlystov, A., Stanier, C., Pandis, S.N., 2004. An Algorithm for Combining Electrical Mobility and Aerodynamic Size Distributions Data when Measuring Ambient Aerosol Special Issue of Aerosol Science and Technology on Findings from the Fine Particulate Matter Supersites Program. Aerosol Science and Technology 38, 229–238. https://doi.org/10.1080/02786820390229543

[33] Dua, S.K., Hopke, P.K., 1996. Hygroscopic Growth of Assorted Indoor Aerosols. Aerosol Science and Technology 24, 151–160.

[34] Huff Hartz, K.E., Tischuk, J.E., Chan, M.N., Chan, C.K., Donahue, N.M., Pandis, S.N., 2006. Cloud condensation nuclei activation of limited solubility organic aerosol. Atmospheric Environment 40, 605 617.

[35] Jimenez, J.L., Canagaratna, M.R., Donahue, N.M., Prevot, A.S.H., Zhang, Q., Kroll, J.H., DeCarlo, P.F., Allan, J.D., Coe, H., Ng, N.L., Aiken, A.C., Docherty, K.S., Ulbrich, I.M., Grieshop, A.P., Robinson, A.L., Duplissy, J., Smith, J.D., Wilson, K.R., Lanz, V.A., Hueglin, C., Sun, Y.L., Tian, J., Laaksonen, A., Raatikainen, T., Rautiainen, J., Vaattovaara, P., Ehn, M., Kulmala, M., Tomlinson, J.M., Collins, D.R., Cubison, M.J., E., Dunlea, J., Huffman, J.A., Onasch, T.B., Alfarra,M.R., Williams, P.I., Bower, K., Kondo, Y., Schneider, J., Drewnick, F., Borrmann, S., Weimer, S., Demerjian, K., Salcedo, D., Cottrell, L., Griffin, R., Takami, A., Miyoshi, T., Hatakeyama, S., Shimono, A., Sun, J.Y., Zhang, Y.M., Dzepina, K., Kimmel, J.R., Sueper, D., Jayne, J.T., Herndon, S.C., Trimborn, A.M., Williams, L.R., Wood, E.C., Middlebrook, A.M., Kolb, C.E., Baltensperger, U., Worsnop, D.R., 2009. Evolution of Organic Aerosols in the Atmosphere. Science 326, 1525– 1529. https://doi.org/10.1126/science.1180353

[36] Shilling, J. E., et al. "Mass spectral evidence that small changes in composition caused by oxidative aging processes alter aerosol CCN properties." The Journal of Physical Chemistry A 111.17 (2007): 3358-3368.

[37] Ren, Jingye, et al. "Using different assumptions of aerosol mixing state and chemical composition to predict CCN concentrations based on field measurements in urban Beijing." Atmospheric Chemistry and Physics 18.9 (2018): 6907-6921.

[38] R. H. Moore, E. D. Ingall, A. Sorooshian, A. Nenes, 2008. Molar mass, surface tension, and droplet growth kinetics of marine organics from measurements of CCN activity. GEOPHYSICAL RESEARCH LETTERS, VOL. 35, L07801, doi:10.1029/2008GL033350, 2008

[39] Seoane, R., Dynarowicz-Latka, P., Miñones, J., Gómez-Serranillos, I., 2001. Mixed Langmuir monolayers of cholesterol and `essential' fatty acids. https://doi.org/10.1007/s003960000453

[40] Li, Yanwei, et al. "Cloud condensation nuclei activity and hygroscopicity of fresh and aged cooking organic aerosol."Atmospheric Environment 176 (2018): 103-109.

[41] Perry's Chemical engineers' handbook, 1984. Sixth edition / prepared by a staff of specialists under the editorial direction of late editor Robert H. Perry; editor, Don W. Green; assistant editor, James O. Maloney. New York: McGraw-Hill, [1984] ©1984.

[42] Flynn, G.L., Shah, Y., Prakongpan, S., Kwan, K.H., Higuchi, W.I., Hofmann, A.F., 1979. Cholesterol Solubility in Organic Solvents. Journal of Pharmaceutical Sciences 68, 1090–1097. https://doi.org/10.1002/jps.2600680908

[43] Shih Chen Wang & Richard C. Flagan (1990) Scanning Electrical Mobility Spectrometer, Aerosol Science and Technology, 13:2, 230-240, DOI: 10.1080/02786829008959441

[44] Tyler J. Johnson, Martin Irwin, Jonathan P. R. Symonds, Jason S. Olfert & Adam M. Boies (2018) Measuring aerosol size distributions with the aerodynamic aerosol classifier, Aerosol Science and Technology, 52:6, 655-665, DOI: 10.1080/02786826.2018.1440063

[45] Liu, H., Cao, G., 2016. Effectiveness of the Young-Laplace equation at nanoscale. Scientific Reports 6, 23936.

[46] Langmuir, I., 1916. THE CONSTITUTION AND FUNDAMENTAL PROPERTIES OF SOLIDS AND LIQUIDS. PART I. SOLIDS. J. Am. Chem. Soc. 38, 2221–2295. https://doi.org/10.1021/ja02268a002

[47] Biskos, G., Russell, L.M., Buseck, P.R., Martin, S.T., n.d. Nanosize effect on the hygroscopic growth factor of aerosol particles. Geophysical Research Letters 33, 2006. https://doi.org/10.1029/2005GL025199

[48] Vazquez, G., Alvarez, E., Navaza, J.M., 1995. Surface Tension of Alcohol Water + Water from 20 to 50 degree. C. Journal of Chemical & Engineering Data 40, 611–614. https://doi.org/10.1021/je00019a016e

[49] Noyes, W.A., Warfel, R.R., 1901. The boiling-point curve for mixtures of ethyl alcohol and water. Journal of the American Chemical Society 23, 463–468. https://doi.org/10.1021/ja02033a004